Heliyon 10 (2024) e37458

Contents lists available at ScienceDirect

Heliyon

journal homepage: www.cell.com/heliyon

Research article

A comprehensive comparison of advanced metaheuristic photovoltaic maximum power tracking algorithms during dynamic and static environmental conditions

AL-Wesabi Ibrahim [a,*], Hassan M. Hussein Farh [b,**], Zhijian Fang [c], Abdullrahman A. Al-Shamma'a [b], Jiazhu Xu [a], Fahad Alaql [b], Walied Alfraidi [b], Muhammad Hamza Zafar [d]

[a] College of Electrical and Information Engineering in Hunan University, Hunan, 410083, China
[b] Electrical Engineering Department, College of Engineering, Imam Mohammad Ibn Saud Islamic University, Saudi Arabia
[c] School of Automation, China University of Geoscience, Wuhan, 430074, China
[d] Department of Engineering Sciences, University of Agder, Grimstad, Norway

ARTICLE INFO

Keywords:
Photovoltaic
MPPT
Dandelion optimizer, metaheuristic approaches
Partial shading scenarios
Uniform irradiances
Static and dynamic environments

ABSTRACT

This study introduces a novel technique for achieving the global peak (GP) in solar photovoltaic (PV) systems under partial shadowing conditions (PSC) using the Dandelion Optimizer Algorithm (DOA), inspired by the dispersal of dandelion seeds in the wind. The proposed approach aims to enhance the power generation efficiency of PV systems across various scenarios, including dynamic uniform, dynamic PSCs, static uniform irradiances, and static PSCs. The proposed approach improves tracking efficiency, provides non-oscillatory steady-state responses, and reduces transients as well as enhancing the dynamic performance of the whole system. Simulation and hardware-in-loop (HIL) experiments demonstrate that the DOA outperforms several state-of-the-art techniques, such as hybrid grey wolf optimizer since-cosine algorithm (HGWOSCA), grasshopper optimization algorithm (GOA), dragonfly optimizer (DFO), particle swarm optimizer with gravitational search (PSOGS), PSO, cuckoo search algorithm (CSA), perturb &observe (P&O), and incremental conductance (INC), achieving average efficiencies of 99.93 %, 88.84 %, 94.48 %, 87.12 %, 88.05 %, 94.79 %, 93.82 %, 85.25 %, and 77.93 %, respectively. These results underscore the DOA's effectiveness in improving maximum power point tracking (MPPT) performance in solar arrays, particularly under challenging dynamic PSC conditions.

1. Introduction

The solar photovoltaic (PV) energy system, recognized for its renewable and environmentally friendly characteristics, stands out as a promising alternative to conventional fuels like natural gas[1–4]. Scientists have been looking for ways to boost the efficiency of solar panels as a result of the growing global trend toward solar energy and the growing interest in solar panels. Photovoltaic cells, which make up solar panels, are what allow sunlight to be converted into electrical energy. Finding the ideal model parameters is also

* Corresponding author.
** Corresponding author.
E-mail addresses: Ibrahim@hnu.edu.cn (A.-W. Ibrahim), hhhussein@imamu.edu.sa (H.M. Hussein Farh).

https://doi.org/10.1016/j.heliyon.2024.e37458
Received 1 May 2024; Received in revised form 29 August 2024; Accepted 4 September 2024
Available online 6 September 2024

necessary for simulation, optimization, and performance assessment of solar systems [5,6]. Despite its advantages, the PV technology encounters nonlinearity in the power-voltage curve due to environmental conditions like temperature and irradiance. The critical point on this curve, known as the maximum power point (MPP), signifies the peak potential output. Maintaining the MPP necessitates the application of a MPPT controller. While conventional MPPT approaches can effectively handle uniform irradiance, PSCs introduce multiple peaks on the power-voltage curve, including one GMPP and several additional local maximum power points. Conventional MPPT approaches, unfortunately, struggle to recognize the global peak during PSCs. Advanced and modern MPPT have been developed to adaptively track the GMPP in case of changing shading conditions, ensuring optimum efficacy in PV systems. Consequently, the pursuit of global power tracking in these PV systems, under both uniform and PSCs, holds significance in enhancing the system's performance concerning output power, efficiency, reliability, and quality[7–9].

Partial shading can significantly impact the performance of PV systems. Several mitigation techniques are proposed to address this issue. These mitigation techniques may be categorized into soft computing techniques and hardware solutions. Soft computing techniques and hardware solutions both play crucial roles in mitigating the impact of PSC on the PV systems. The review of the state-of-the-art examines hybrid, traditional, and soft computing methods for mitigating shadowing in solar applications. It offers a thorough rundown of shade mitigation with various topologies. In soft computing techniques, such as PSO and modified current sensor-less approaches, have been shown to effectively handle partial shading conditions. These techniques offer robustness, flexibility, and reliability, making them highly suitable for addressing the challenges posed by partial shading in PV systems[10–12].

In contrast, hardware based-solutions, including module-level and array-level techniques, involve physical reconfigurations of the PV system to minimize the effects of PSCs [13]. On the other hand, a literature review of partial shading mitigation approaches reveals various hardware and theoretical solutions. One study examines hardware solutions aimed at addressing partial shading issues in grid-connected PV systems, emphasizing both module-level and array-level strategies to mitigate partial shading effects by repositioning modules within the array. Meanwhile, another extensive review delves into the theoretical underpinnings of reverse breakdown mechanisms in PV cells/systems, exploring diverse techniques to alleviate the impact of partial shading on the performance of PV systems. These hardware solutions often require additional components and complex reconfigurations to achieve shading mitigation. While both soft computing techniques and hardware solutions have their advantages, soft computing techniques are favored due to their capacity to precisely track the maximum power point of PV systems, particularly in scenarios involving partial shading [14–18].

In the past few decades, researchers have worked to improve solar photovoltaic (PV) system performance. As part of this effort, many maximum powers point tracking (MPPT) controllers have been designed at various points in time [19,20]. The most fundamental and early approaches are known as conventional MPPT methods, and they include perturb and observe (P&O) [21,22], incremental conductance [18,23]. In addition to conventional algorithms, there are many more solutions available, such as bioinspired algorithms, which are substantially more efficient in some particular instances than conventional ones[24–26]. They are capable of rapidly converging to a global maximum and hence can save power loss even in a partially changed environment [27]. Generally, PSO has several benefits, such as its straightforward installation and its capacity to explore large, intricate search areas quickly. That might, however, have the disadvantage of being trapped in local optima, producing less-than-ideal results [28–30]. Not only that, but PSO can have a delayed convergence rate especially when dealing with high-dimensional problems and premature convergence. However, CSA is well-known for its efficient exploration and exploitation skills, which make it appropriate for jobs involving global optimization. However, there are several drawbacks to CSA [31]. One significant problem is that it heavily relies on randomization, which can cause unanticipated fluctuations in the output signal and compromise the optimization process's stability and convergence. In addition, CSA could show slower rates of convergence when compared to other algorithms. The probabilistic selection of potential solutions is a feature shared by the artificial bee colony (ABC) and moth flame optimizer (MFO) methods [32]. Although this random aspect permits the search space to be explored, it may result in undesired oscillations in the output. Noteworthy power losses and reduced energy output in the PV panels may arise from these oscillations at the GMPP. Therefore, in situations when a steady and smooth output is essential, such in continuous MPPT monitoring, ABC and MFO might not be sufficient. The GMPP is effectively followed by the grey wolf optimizer (GWO), which performs best in clear sky circumstances. In overcast PV system settings, nevertheless, it can face difficulties. Grey wolves travel slowly over the search space as the tuning value decreases over time, requiring additional iterations. Due to trapping the LMPP, which occurs when an algorithm is trapped in a local optimum, GMPP tracking may be delayed and the system's ability to capture the ideal power output may be undermined. However, even in the presence of PSCs, the grasshopper optimization algorithm (GOA) shows encouraging capabilities in terms of GMPP monitoring. It can stabilize the output power and adjust to changing situations with effectiveness. On the other hand, the output power at the GMPP might casually oscillate due to the tuning limits included in GOA. These oscillations can nevertheless affect the total power generation and cause some power losses, even if they are not as bad as the unwanted variations observed in ABC and MFO [33].

Finally, great consideration should be given to the climatic circumstances and system requirements when selecting an optimization strategy for MPPT in PV modules. With the shortcomings of previous approaches eliminated, this study offers a fresh approach to PV-system MPPT control. The dandelion optimizer algorithm (DOA), a swarm intelligence bio-inspired metaheuristic algorithm, is applied in this method to improve GMPP tracking [29]. The DOA is notable for using a novel method to simulate the flight dynamics of dandelion seeds in three steps: ascent, descent, and landing. Random trajectories are added throughout the rising stage to enable simple adaptation to varying weather conditions. The landing step of the method uses a linear rising function in conjunction with Levy flight, whereas the descending stage uses a Brownian motion trajectory. DOA can attain a healthy balance between exploration and exploitation because of its ingenious blend of trajectory patterns. This balancing greatly improves the accuracy and efficiency of identifying the GMPP in a variety of dynamic situations and weather conditions. Using this cutting-edge modeling technique, DOA becomes a viable and cutting-edge MPPT option for PV systems. It is a dependable and effective option for maximizing energy harvesting in PV systems due to its flexibility to adjust to changing conditions and its effective power tracking capabilities [34].

The above literature collectively offers insights into the challenges posed by partial shading in PV systems and the various hardware and theoretical techniques proposed to mitigate its impact. The soft computing techniques offer a more adaptable and efficient approach to addressing the challenges posed by partial shading, making them a valuable complement to hardware solutions in the field of photovoltaic applications. The literature emphasizes the critical need for developing robust mitigation strategies to improve both the performance and reliability of grid-connected PV systems, especially when confronted with partial shading conditions. As was previously indicated, several optimization techniques have limits when it comes to measuring MPP for PV systems, despite being frequently employed. Inspired by the dandelion plants disperse, DOA is a viable alternative. It is a great contender for MPPT algorithms in solar systems due to its distinctive properties. Table 1 presents a thorough analysis of DOA's performance in relation to current optimization strategies. The goal of this research is to fully explore DOA's potential for MPPTs in solar power systems.

This study introduces the Dandelion Optimizer Algorithm (DOA), a novel optimization method designed to find the GMPP of solar PV systems. The DOA leverages advanced mathematical techniques to optimize the system's operating point, ensuring high efficiency in both static and dynamic conditions. The key contributions of this work are:

- Development of the DOA: The proposed DOA enhances the efficiency of PV systems by ensuring rapid and reliable convergence, thanks to reinitializations and the elimination of random interacting effects.
- Comparative Analysis: A detailed comparison with eight established benchmark algorithms (HGWOSCO, GOA, DFO, PSOGS, PSO, CSA, P&O, and INC) is conducted. The performance of these algorithms is assessed using metrics such as robustness, accuracy, and convergence speed. The findings indicate that the DOA outperforms these benchmarks, suggesting its superiority for MPPT optimization in PV systems.
- Validation through Experiments: Extensive simulations and practical experiments validate the efficacy and robustness of the DOA methodology. This validation includes scenarios with highly variable PV radiation and partial shading conditions. The practical feasibility of implementing the DOA and other methods is further confirmed through Hardware-in-Loop (HIL) testing.

These contributions underscore the DOA's significant advancement in improving the performance of PV systems under challenging conditions, making it a viable optimization strategy for real-world applications.

The subsequent sections of this paper are structured as follows: Section 2 outlines the solar cell modeling, while Section 3 delves into the implications and characteristics of partial shading. The innovative DOA is elaborated upon in Section 4, followed by the presentation of simulation and experimental results in Sections 5 and 6, respectively. Section 7 evaluates the performance of the Maximum Power Point Tracking (MPPT) algorithms, concluding with Section 8.where, L is Low, VL is Very Low, M is Medium, H is High and VH is Very High.

2. Description of the PV energy conversion system

Fig. 1 illustrates the PV energy system, where the PV array connects to the load via a DC-DC converter (boost). Inputs to the PV array include irradiance (W/m^2) and temperature (^{o}C). The energy conversion system comprises three interconnected PV modules, with series PV modules receiving identical irradiance inputs. Table 2 lists specifications/parameters of the PV module; Tata Power Solar System TP250MBZ; utilized in this investigation. The power output is determined by multiplying the PV voltage (V_{PV}) and current (I_{PV}). This resultant power output serves as the input for the MPPT algorithm, which calculates the optimal duty cycle (D) for the step-up converter. The DC-DC boost converter increases voltage while decreasing current from its input (source) to its output (load). Table 3 lists the specifications/parameters for the boost converter. The step-up converter is regulated to operate based on the value of D, allowing for the tracking of the maximum power point (MPP) by controlling the duty ratio of the boost converter.

A photovoltaic cell is comprised of a light source that generates electricity, a diode linked in parallel, and a series resistance. PV panels, which may be connected in parallel or series to produce the required power output, are typically assembled from these PV cells. The ideal PV cell may consist of a DC source with an anti-parallel diode. Resistance, such as series resistance (Rs) and shunt resistance (Rp), must be added, though, as Fig. 2 illustrates, in order to make the model more useful. A practical single-diode mode's

Table 1
Comparative analysis of recently published metaheuristic algorithms based on MPPT.

Algorithms	Year	Convergence Speed	Tracking Efficiency	Implementation Complexity	Power losses	Oscillation
GWO [35]	2016	L	H	H	M	M
ACO [36]	2017	M	M	M	M	L
PSO [37–40]	2018	H	H	H	H	L
BA [41]	2020	M	H	H	M	M
GOA [42]	2020	H	H	H	M	L
CSA [43]	2021	L	L	M	H	L
ABC [44]	2021	H	H	H	M	L
CSA [31]	2022	L	L	M	M	L
DO [29]	2023	H	VH	M	L	VL
DO [34]	2023	H	H	M	L	L
Proposed DOA	2024	V	VH	M	VL	VL

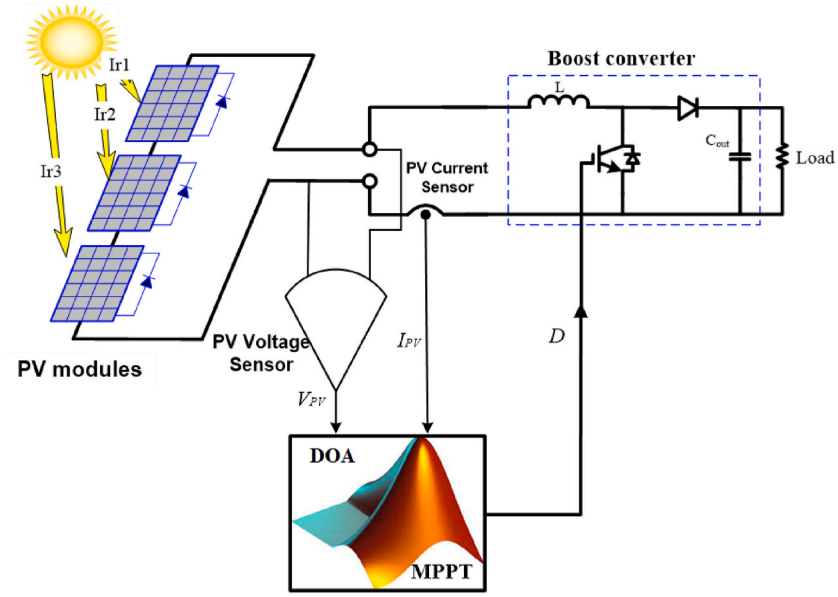

Fig. 1. The PV energy conversion system modeling.

Table 2
The PV module electrical parameters for the Tata Power Solar Systems TP250MBZ.

Parameter	Value
Maximum power for each module (W)	249 W
$V_{o.c}$ (V)	36.5 V
Cells per module (N_{cell})	60
$I_{S.C}$ (A)	8.83 A
Maximum voltage power point (V)	30.2 V
Maximum current power point (A)	8.30 A
Light-generated current (A)	8.83 A
Diode saturation current (A)	1.0132–10
Diode ideality factor	0.94812

Table 3
Technical parameters and specifications of the boost converter.

Component	Description	Specifications
Switching Frequency	*f*	50 kHz
Boost inductor	*L*	1.14 mH
Output capacitor	*C2*	0,47 mF
Input capacitor	*C1*	10 μF
Resistive load	*R*	14 Ω
IGBT + Diode	*SKM*50GAL	1200 V, 50 A
IGBT Driver	*SKHI 10/12R*	1200 V, 8 A

mathematical expression can be found in Ref. [45].

3. Partial shading effects

Partial shading can significantly alter the power-voltage (P-V) curve of a PV module, depicting the relationship between output power and voltage under varying solar irradiance levels. Under unshaded conditions, the P-V curve exhibits a distinct shape with a single maximum power point (MPP) representing the module's optimal operating point. However, partial shading alters this curve, leading to multiple MPPs and potential power losses. Identifying the optimal operating point becomes challenging as the MPP shifts from a single point to a range of positions. Additionally, shaded cells may experience reverse biasing, potentially causing cell deterioration and the formation of hotspots that can permanently damage the module.

Fig. 3a depicts the scenario where all solar panels receive uniform irradiance of 1000 W/m^2, resulting in P-V and I-V curves with a

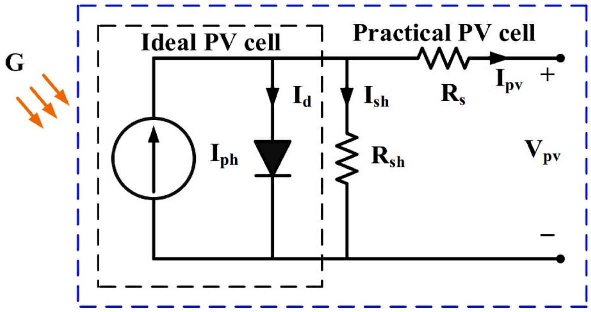

Fig. 2. The single-diode PV cell model.

single maximum power point (MPP). In contrast, Fig. 3b illustrates partial shading (PS) conditions, where irradiance levels vary across panels (1000 W/m^2, 700 W/m^2, 600 W/m^2, and 400 W/m^2), leading to multiple local peaks (LPs) and a single global peak (GP) in the P-V and I-V curves. Managing MPPT becomes complex under partial shading to ensure optimal power output despite varying irradiance and weather conditions.

4. Applied metaheuristic MPPT techniques

MPPT, or Maximum Power Point Tracking, is a crucial strategy employed in solar energy systems to optimize the output of solar panels by continuously adjusting the operating point to the maximum power point. Various MPPT methods exist to enhance the power output of PV systems, with the choice depending on factors such as required accuracy, computational resources, and environmental conditions. This study employs a range of MPPT methods including Hybrid Grey Wolf Optimizer Since-Cosine Algorithm (HG-WOSCA), Cuckoo Search Algorithm (CSA), Particle Swarm Optimization (PSO), Grasshopper Optimization (GOA), Dragonfly Optimization (DFO), Particle Swarm Optimization with Gravitational Search (PSOGS), and Modified Incremental Conductance.

4.1. Implementing dandelion optimizer algorithm as MPPT

2022 saw the introduction by Shijie Zhao of a very successful worldwide optimization technique that, as Fig. 4 illustrates, makes use of the mechanism by which wind disperses dandelion seeds over great distances. The technique achieves more rapid convergence rates on worldwide smooth problems than earlier approaches that only made use of the function's local smoothness. It has been

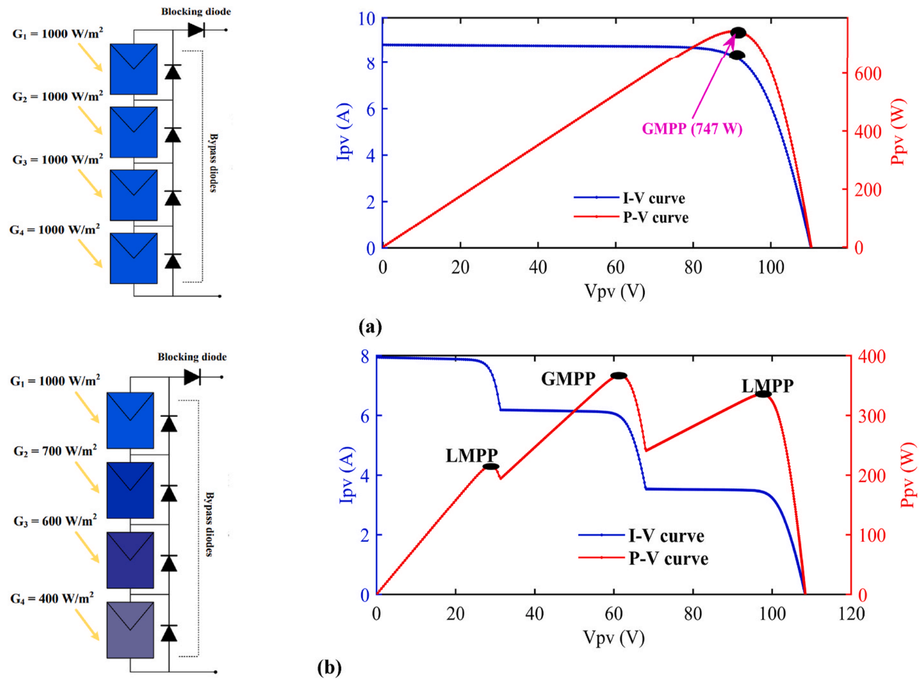

Fig. 3. The P-V and I-V characteristics of PV modules during (a) uniform radiation; (b) nonuniform radiation; PSCs.

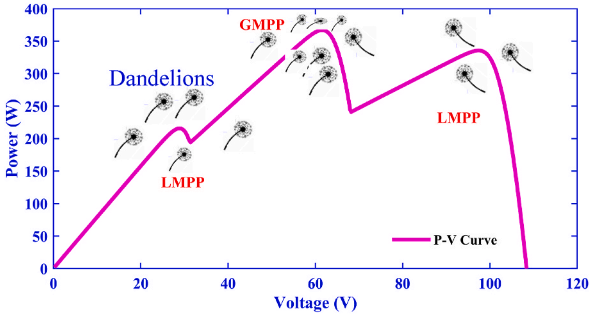

Fig. 4. Dandelion flowers carried by the wind in search of the Global Maximum Power Point (GMPP).

mathematically demonstrated that this method performs better than a simple random searches algorithm and produces amazing results [46]. The dandelion optimization procedure relies on the dispersion of dandelion seeds by the wind, enabling them to inhabit new surroundings and adjust to evolving conditions. In a parallel manner, the DOA produces numerous solutions and investigates various regions within the solution space through the incorporation of randomness and variability, aiming to discover the most optimal solution [46].

4.1.1. DOA mathematical model

The DOA iterates through the wind and replication operators until it reaches an end criterion, such as achieving an acceptable level of fitness or reaching a maximum iterations number. The ultimate solution selected by the technique is the top answer identified during the optimization phase. This section delves into the mathematical formulas associated with DOA.

1) Initialization

DOA uses evolution of populations and iterative optimization based on population initiation, or seed generation, just like other nature-inspired metaheuristic techniques. The process in the suggested MPPT-based DOA produces a few duty ratio of step-up converters (D), that stand in for possible solutions to our optimization issues. The population is shown as Eq. (1):

$$Population = \begin{bmatrix} d_1 \\ \vdots \\ \vdots \\ d_{Pop} \end{bmatrix} \tag{1}$$

where pop denotes the size of the population.

Among the upper bound (U_b) and lower bound (L_b), each possible solution is created at random, and the expression of the i_{th} individual d_i is shown in Eq. (2):

$$d_i = rand \times (\mathrm{U}_b - \mathrm{L}_b) + \mathrm{L} \tag{2}$$

where an integer between 1 and pop is represented by the symbol i, and rand is a random number between zero and one.

The first elite the participant with the highest fitness value is determined by DOA during the initialization phase. This is said to be the ideal place for a dandelion seed to germinate and grow. Next, we define the mathematical formulation of the initial elite (d_{elite}) as follows: where two equal-valued indices are referenced by the function find(.) as shown in Eq. (3).

$$\begin{aligned} f_{best} &= \min(f\mathrm{d}_i) \\ \mathrm{d}_{elite} &= d(find(f_{best} = f(\mathrm{d}_i))) \end{aligned} \tag{3}$$

2) Rising Stage

In the rising stage, dandelion seeds need to reach an appropriate height before they may separate from their parent by floating. The height at which dandelion seeds rise varies based on many parameters such air humidity and wind velocity. In this instance, there are two categories of climate.

The first scenario It is reasonable to suppose that wind speeds follow a lognormal distribution on a clear day. In order to explore new areas of the search space and find novel probable solutions that are superior to the best one currently in place, dandelion seeds are more likely to travel to far-off regions along the Y-axis, where random numbers are more spread in this distribution. The dandelion flies soar higher and the seeds spread farther with increasing wind speed. The wind speed continuously modifies the vortexes above the dandelion seeds, causing them to rise in a spiral pattern. The matching mathematical formula in this instance is shown in Eq. (4):

$$d_{k+1} = d_k + \left(\alpha \times v_x \times v_y \times \ln Y \times (d_s - d_k)\right) \tag{4}$$

where v_x and v_y are defined in Eq. (5)

$$\begin{aligned} v_x &= r\cos\theta \\ v_y &= r\sin\theta \end{aligned} \tag{5}$$

where r in Eq. (6) is the random parameter and θ is a random parameter in the interval $[-\pi, \pi]$:

$$r = \frac{1}{e^{\theta}} \tag{6}$$

where d_s is the random selected location in the searching region throughout iteration k, whereas d_k is the initial position of the dandelion seed throughout iteration k. Eq. (7) is the expression for the position that is created randomly:

$$d_s = rand(1,1) \times (U_b - L_b) + U_b \tag{7}$$

The lognormal distribution equation, or lnY, is as Eq. (8):

$$\ln Y = \begin{cases} \frac{1}{y\sqrt{2\pi}} \exp\left[-\frac{1}{2\delta^2}(\ln y)^2\right] & y \geq 0 \\ 0 \quad y < 0 \end{cases} \tag{8}$$

where lnY denotes the standard normal distribution $N(0, 1)$ in Eq. (8) and lnY denotes a lognormal distribution according to $\mu = 0$ and $\delta^2 = 1$. The mathematical expression for α, an adaptive parameter that modifies the length of the search step, is as Eq. (9):

$$\alpha = rand() \times \left(\frac{1}{k_{\max}^2}k^2 - \frac{2}{k_{\max}}k + 1\right) \tag{9}$$

The second scenario: When it rains, air resistance and humidity prevent dandelion seeds from being transported away by the wind, causing them to remain in their immediate vicinity. This can be expressed mathematically as Eq. (10):

$$d_{k+1} = d_k \times T \tag{10}$$

At the end of each iteration, the parameter T slowly approaches 1, controlling the dandelion's local search range. This adjustment ensures that the population settles on the optimum search agent. To compute the domain, use Eq. (11):

$$T = 1 - rand \times q \tag{11}$$

where the value of q is given as Eq. (12):

$$q = \left(\left(\frac{1}{k_{\max}^2 - 2k_{\max} + 1}k^2\right) - \left(\frac{2}{k_{\max}^2 - 2k_{\max} + 1}k + 1\right) + \left(\frac{1}{k_{\max}^2 - 2k_{\max} + 1}\right)\right) \tag{12}$$

In summary, Eq. (13) is the mathematical expression for dandelion seeds through the rising stage:

$$d_{k+1} = \begin{cases} (d_k + \alpha \times v_x \times v_y \times \ln Y \times (d_s - d_k)) & \text{randn} < 1.5 \\ d_k + T \quad \text{Else} \end{cases} \tag{13}$$

A typical distribution of random numbers (*randn*) is used by the DOA technique to continuously change the ratio of exploration to exploitation. To improve the approach's global search direction, a cutoff point of 0.5 is chosen. Because of this, the initial stage of iterative optimization can utilize dandelion seeds to investigate the entire search space, pointing the subsequent stages of the procedure in the appropriate directions.

3) Descending Stage

The DOA strategy prioritizes exploration during this phase, employing Brownian motion to simulate the descent of dandelion seeds after reaching a certain height. As Brownian motion adheres to a normal distribution, it enables exploration across a wider range of search spaces during the iteration process. Additionally, the DOA technique utilizes average position data post-upward movement to gauge the stability of the seed's descent, guiding the population towards more favorable regions. Mathematically, this process can be represented as Eq. (14):

$$d_{k+1} = d_k - (\alpha \times \beta_k \times (d_{mean\_k} - \alpha \times \beta \times d_k)) \tag{14}$$

where β_k represents the Brownian motion and is a random number taken from the typical distribution.

The average position of the population in the i_{th} iteration is denoted by d_{mean_k}, and its mathematical expression is as Eq. (15):

$$d_{mean\_k} = \frac{1}{Pop}\sum_{i=1}^{Pop} d_i \tag{15}$$

4) Land Stage

The outcomes of the first two steps determine the landing site that the dandelion seed chooses during the exploitation phase of the DOA strategy. The method aims to arrive at the global optimal solution through repeated iterations. Eq. (16) is a representation of this process.

$$d_{k+1} = d_{elite} + (Levy(\lambda) \times \alpha \times (d_{elite} - d_k \times \delta)) \tag{16}$$

where d_{elite} represents the ideal location of the dandelion seed in the i_{th} iteration. Eq. (16) may be used to produce levy(λ), which is the Levy flight function, and Eq. (17) can be used to calculate σ, which is a linear growing function between [0, 2].

$$Levy(\lambda) = s \times \frac{\omega \times \sigma}{|t|^{\frac{1}{\beta}}} \tag{17}$$

And

$$\delta = \frac{2t}{T} \tag{18}$$

In Eq. (18), δ, a random parameter between [0, 2], is employed. In this study, s is a fixed constant of 0.01 while $\beta = 1.5$, ω, and t are random values between zero and one. σ has the following mathematical expression as Eq. (19):

$$\sigma = \left(\frac{\Gamma(1+\beta)\sin\left(\frac{\pi\beta}{2}\right)}{\Gamma\left(\frac{1+\beta}{2}\right)\beta 2^{\left(\frac{\beta-1}{2}\right)}} \right) \tag{19}$$

5) Convergence determination

The rising, lowering, and landing phases of the iterative optimization process are how the DOA technique works. Because the duty ratios follow random trajectories during the rising stage, a thorough search space investigation can be conducted to find possible optimal spots. The Brownian motion trajectory is used in the descending stage to fine-tune the optimization procedure, concentrating on potential areas inside the search space. Lastly, in order to optimize the duty ratios and go closer to the GMPP, the landing stage makes use of a linear rising function with Levy flight.

6) Re-initialization

The fitness value of the MPPT, which uses temporal variant optimization, frequently varies based on the climate conditions. In these situations, the duty ratios, or positions of the DOAs, are reinitialized to look for the new GMPP once more. In this article, the following constraint equation is used to detect changes in SP or insolation and reinitialize the duty ratios as Eq. (20):

$$\frac{P_{PV}^{k+1} - P_{PV}^{k}}{P_{PV}^{k+1}} \geq \Delta P\% \tag{20}$$

4.2. The DOA Technique's execution for MPPT

To guarantee the efficient and precise functioning of the DOA method in PV systems, several limitations and adjustments must be made when applying it to MPPT.

Initializing and Constraints of the Duty Ratio: In the naturalistic analogy, the duty ratios in the DOA technique translate into control signals that are sent to the converter, just like dandelion seeds. The maximum value ($d_{\max} = 0.9$) and the minimum value ($d_{\min} = 0.1$) restrict the search space where the duty ratios are required to be initialized before the optimization procedure can start. These limitations serve to limit the optimization to a safe and practical range of duty cycles that don't result in instability or go beyond the converter's operating parameters. This guarantees that the method begins with power conversion values that are sensible and does not start with any hazardous or unfeasible settings.

Three steps make up the iterative optimization process that the DOA methodology uses to go forward: rising, lowering, and landing. In the upward phase, the duty ratios follow stochastic paths, which facilitate a wide range of searches to find possible best spots. In order to fine-tune the optimization procedure and concentrate on promising areas within the search space, the descending step uses the

Brownian motion trajectory. To fine-tune the duty ratios and move closer to the GMPP, the landing stage finally applies a linear rising function with Levy flight.

4.2.1. Purpose of DOA in MPPT

The primary purpose of the DOA in the context of MPPT for photovoltaic (PV) systems is to efficiently and accurately identify the GMPP under various environmental conditions. The DOA is inspired by the natural dispersal mechanism of dandelion seeds, which ensures widespread exploration of the search space and robust convergence to the optimal solution.

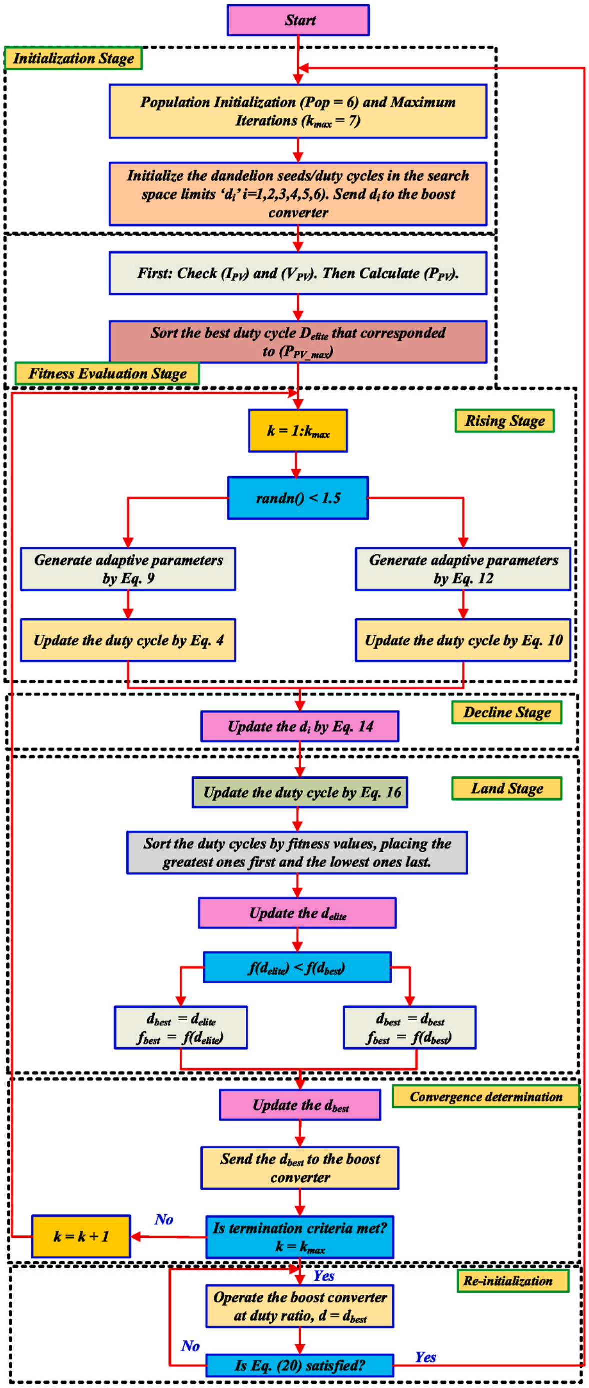

Fig. 5. The DOA Flowchart based-MPPT for PV modules.

4.2.2. Objectives of the DOA in MPPT

Enhanced Tracking Accuracy: The DOA aims to improve the precision with which the MPPT controller can track the GMPP. This is particularly important in PSC where multiple local maxima may exist. The algorithm's ability to distinguish between local and global maxima ensures that the PV system consistently operates at its highest possible efficiency.

Rapid Convergence: One of the critical challenges in MPPT is the need for rapid adaptation to changing irradiance levels and shading patterns. The DOA is designed to achieve swift convergence to the GMPP, minimizing the time the PV system spends in suboptimal operating points. This quick response is vital for maintaining high energy yield, especially in dynamic environments.

Stability and Reliability: The DOA provides a stable and reliable MPPT method that can handle fluctuations in environmental conditions without causing oscillations or instability in the power output. Stability is crucial for ensuring the longevity and safety of the PV system components.

Finding the optimal Duty Ratio: The DOA methodology iteratively adjusts the duty ratio positions until it reaches convergence, at which time the ideal duty ratio that represents the GMPP is found. After that, the converter receives this duty ratio and modifies the power conversion to run at the PV system's ideal power output. A Flowchart depicting the sequential execution of the DOA method under PS conditions is shown in Fig. 5. A visual depiction of the algorithm's progression through the many steps, including altering duty ratios and obtaining the GMPP, is given by the flowchart. This pseudocode for the DOA is as follows:

1. Initialize the population of dandelion seeds (solutions) *for i = 1 to N do* *Initialize seed_i with a random position within the search space* *end for* *2. Evaluate the fitness of each seed* *for i = 1 to N do* *Compute the fitness of seed_i based on the PV system's power output* *end for* *3. Identify the initial global best solution (global_best)* *global_best = seed with the highest fitness*	*7. Evaluate the fitness of the new seed* *new_fitness = compute_fitness(new_seed)* *8. if (new_fitness > current_fitness of seed_i) then* *9. Replace seed_i with new_seed* *seed_i = new_seed* *end if* *end for* *10. Update the global best solution* *current_best = seed with the highest fitness in the population* *if (current_best fitness > global_best fitness) then*
4. while (termination criteria not met) do *5. for each seed in the population do* *6. Select a neighboring seed based on dandelion dispersal pattern* *new_seed = generate_new_seed(seed_i)*	*global_best = current_best* *end if* *end while* *11. Return the global best solution as the MPP*

5. Simulation results and discussion

5.1. Simulation study under static and dynamic environments

Case 1. Static Uniform Conditions

Under uniform conditions, all solar PV modules receive the same quantity of sunlight, resulting in a single peak. The radiation applied to the three PV modules are identical [1000,1000,1000], and the PV output power and PV voltage values at the MPP are 747 W and 90 V as demonstrated in Fig. 6.

In the first experiment, the PV modules get a constant 1000 W/m^2. The findings demonstrate that when compared to other

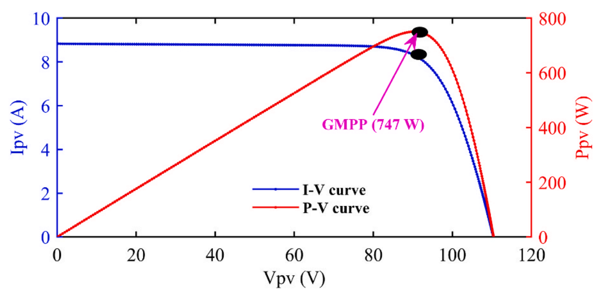

Fig. 6. The P-V and I-V characteristics under the first scenario.

methods, DOA has a substantially shorter convergence time and minimal size variations. Moreover, Fig. 7a illustrates how well DOA tracks the MPP of 747 W, using a voltage of 149.7 V and a current of 4.99 A at MPP to achieve 100.00 % tracking efficiency with a recorded converging time of 0.18 s. Conversely, Fig. 7b shows that DOA exhibits a significantly faster settling time than HGWOSCO, which can follow the MPP adequately and has a tracking time of only 0.27 s. With a voltage of 149.5 V and a current of 4.99 A at MPP, it settles at a lesser value of 746.96 W and achieves an efficiency of 99.98 %. GOA, DFO, PSOGS, PSO, CSA P&O, and INC (Fig. 7c–i) can follow the MPP oscillations and extended time with success. Its increased steady-state oscillations cause power losses and lower efficiency, and it takes longer to settle than DOA and HGWOSCO. In terms of settling time, DOA exhibits an improvement over GOA, DFO, PSOGS, PSO, CSA P&O, and INC. Notably, DOA performs better in fully insolated situations; however, partial shading scenarios should be well-suited for the metaheuristic method. Table 4 presents a comparison of the results obtained in terms of power, tracking time, and efficiency during case one.

Case 2. Static Partial Shading Conditions

Under static PSCs, all solar PV modules receive different quantity of irradiance, resulting in multiple power peaks (unique global

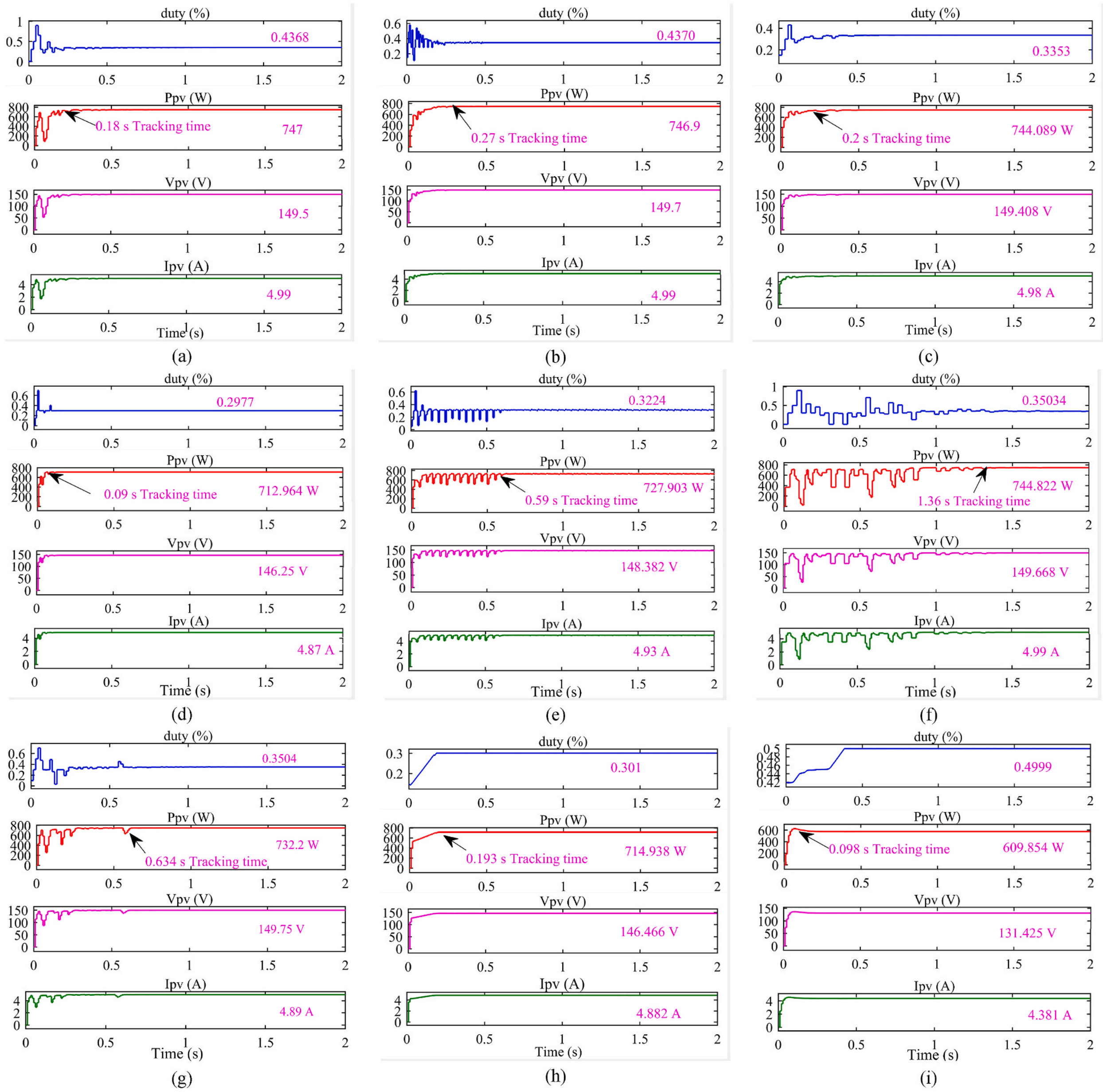

Fig. 7. The PV modules output characteristics during static uniform weather conditions [1000, 1000, 1000]: a) DOA, and b) HGWOSCO, c) GOA, d) DFO, e) PSOGS, f) PSO, g) CSA, h) P&O and i) INC.

Table 4
Comparisons between the obtained results under static uniform conditions (Case one).

Algorithm	Theoretical power (P_{th})	Measure power (W)	Tracking time (s)	Efficiency (%)
DOA	747 W	747	0.18	100.00
HGWOSCO		746.9	0.27	99.98
GOA		744.089	0.2	99.61
DFO		712.964	0.09	95.44
PSOGS		727.903	0.59	97.44
PSO		744.822	1.36	99.70
CSA		732.2	0.634	98.01
P&O		714.938	0.193	95.70
INC		609.854	0.098	81.64

and many local peaks). In this case, the irradiances applied to the three PV modules are [1000, 900, 800] causes multiple peaks, the theoretical global peak value at 637.9 W at V_{MPP} 93.4 V based on the power-voltage curve depicted in Fig. 8.

In the second experiment, the radiation values of the four solar panel modules are 800, 900, and 1000 W/m^2, respectively. With a voltage of 138.22 V at MPP and a current of 4.6077 A at MPP, displayed in Fig. 9a, DOA successfully monitors the MPP of 637.872 W in a tracking time of 0.22 s, reaching an efficiency of nearly 99.99 % during the PS circumstance. Fig. 9b demonstrates that GOA achieves a slightly shorter tracking time of 0.24 s, reaching a lower MPP value of 637.2 W, with corresponding voltage and current values at MPP of 138.268 V and 4.60 A, respectively, along with a lower efficiency of 99.89 %. Meanwhile, HGWOSCO, DFO, PSOGS, PSO, CSA P&O, and INC (as shown in Fig. 9-c-i) successfully track MPP fluctuations over an extended duration. Compared to DOA and GOA, it takes more to settle and has higher steady-state oscillations that result in power losses and decreased efficiency. In terms of settling time, DOA shows a notable improvement over HGWOSCO, DFO, PSOGS, PSO, CSA P&O, and INC. These findings indicate that DOA is superior to rival approaches in many ways, most notably in terms of efficiency and the rate of convergence improvement. The proposed technique's resilience in managing static partial shading is amply demonstrated. As a crucial prerequisite for attaining high efficiency and performance in PV systems, our findings show how well the DOA-based MPPT techniques tracks the MPP during varying solar radiation circumstances. Table 5 shows the comparison between the obtained results in terms of the power, tracking time and efficiency during case two.

Case 3. Dynamic Nonuniform Conditions

Under dynamic uniform conditions, the solar PV modules receive the same quantity of uniform irradiances [1000, 1000, 1000] for a certain period [0–1 s] as depicted in Fig. 10a, resulting in one global peak with theoretical power and voltage values of 747 W and 90 V as depicted in Fig. 10b. After that the irradiances have been changed to be [850,850, 850] for intervals from [1–2 s] causes the change in irradiances to another global peak with theoretical power and voltage values of 637 W and 90.5 V as depicted in Fig. 10a,b.

In the third experiment, As shown in Fig. 11a at the PS1[1000, 1000, 1000], DOA successfully monitors the MPP of 747 W in a tracking time of 0.1 s, reaching an efficiency of approximately 100.00 % during the PS scenario 1 with a voltage of 146.25 V at MPP and a current of 4.87 A at MPP and at PS2[850,850, 850], DOA successfully monitors the MPP of 637 W in a tracking time of 1.0 s, reaching an efficiency of approximately 100.00 % during the PS scenario 2 with a voltage of 138.335 V at MPP and a current of 4.61 A. GOA takes longer to reach the MPP, with a tracking time of 0.39 s, settling at a lower value of 743.9 W with a current of 4.97 A at MPP and voltage of 149.3 V at MPP, resulting in an efficiency of 99.58 % at PS1[1000, 1000, 1000]. Meanwhile, GOA at PS2[850,850, 850] obtained 612.76 W power, 135.6 V voltage, and 4.5 A current with a tracking time of 1.03 s, achieving 96.19 % efficiency, as seen in Fig. 11b. HGWOSCO, DFO, PSOGS, PSO, CSA P&O, and INC (Fig. 11c–i) are successful in tracing the MPP fluctuations over an extended time. Compared to DOA and GOA, it takes more to settle and has higher steady-state oscillations that cause losses in power and decreased efficiency. In terms of settling time, DOA shows a notable improvement over HGWOSCO, DFO, PSOGS, PSO, CSA P&O, and INC. These findings indicate that DOA is superior to rival approaches in many ways, most notably in terms of efficiency and the rate of convergence improvement. Table 6 shows the comparison between the obtained results in terms of the power, tracking time and efficiency during case three.

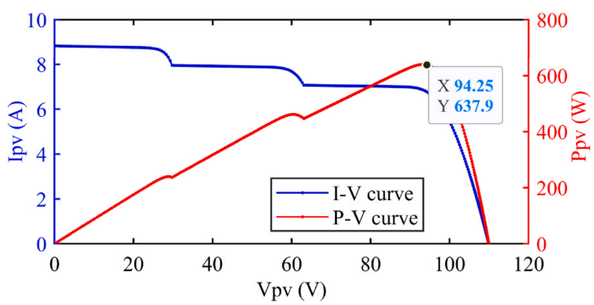

Fig. 8. The P-V and I-V characteristics under the second scenario.

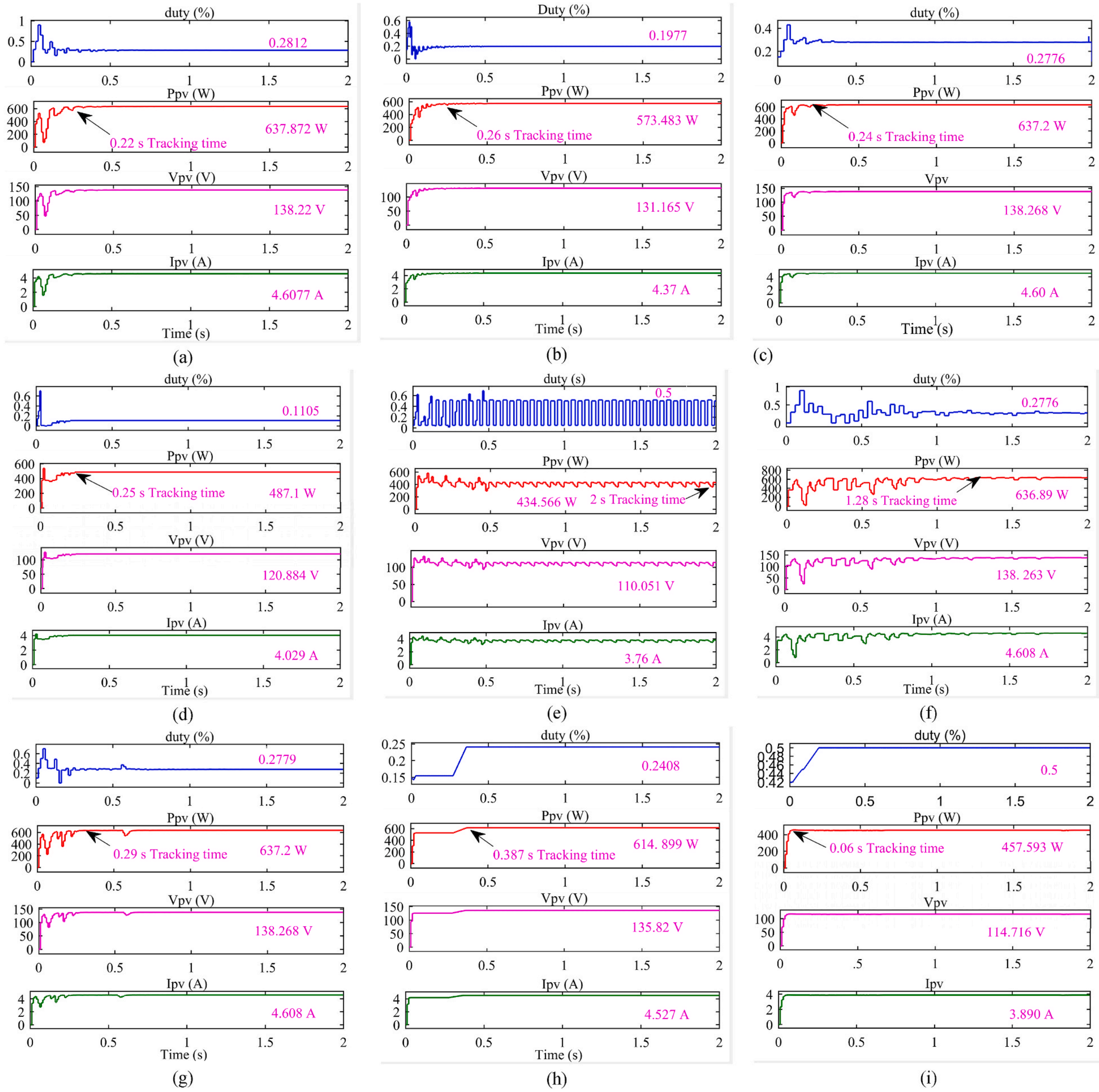

Fig. 9. The PV modules output characteristics during static PSCs [1000, 900, 800]: a) DOA, and b) HGWOSCO, c) GOA, d) DFO, e) PSOGS, f) PSO, g) CSA, h) P&O and i) INC.

Table 5
Comparisons between the obtained results under static partial shading conditions (Case two).

Algorithm	Theoretical power (P_{th})	Measure power (W)	Tracking time (s)	Efficiency (%)
DOA	637.9 W	637.872	0.22	99.99
HGWOSCO		573.483	0.26	89.90
GOA		637.2	0.24	99.89
DFO		487.1	0.25	76.44
PSOGS		434.566	2	68.12
PSO		636.89	1.28	99.84
CSA		637.2	0.29	99.89
P&O		614.899	0.387	96.39
INC		457.593	0.06	71.73

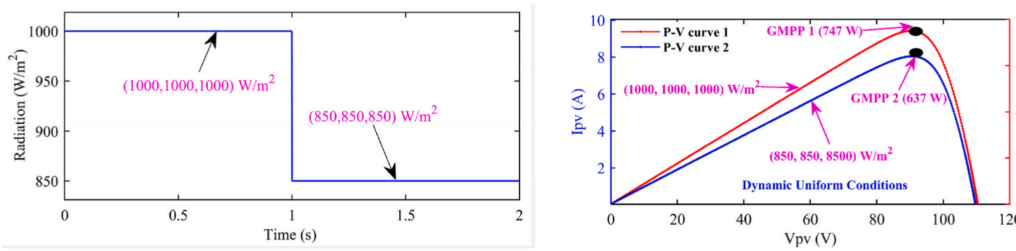

Fig. 10. P-V plots were obtained under condition 3: (a) Radiations profiles, (b) P-V power curves.

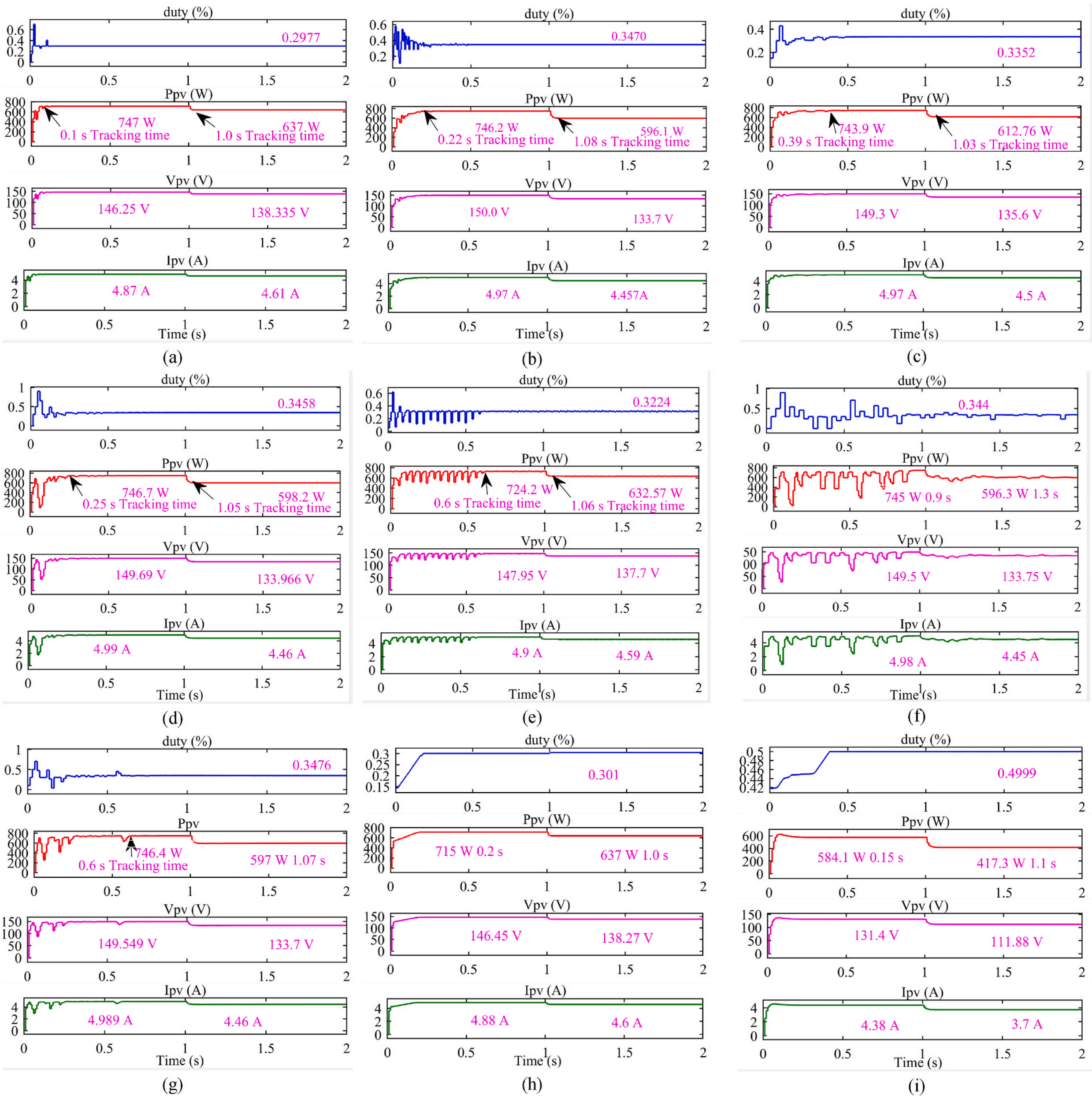

Fig. 11. The PV modules output characteristics during dynamic uniform conditions [1000,1000,1000] and [850,850,850]: a) DOA, and b) HGWOSCO, c) GOA, d) DFO, e) PSOGS, f) PSO, g) CSA, h) P&O and i) INC.

Table 6
Comparisons between the obtained results under dynamic non-uniform conditions (Case three).

Algorithm	First Interval (0–1 s)		Measure power (W)	Track time (s)	Efficiency (%)	Second Interval (1–2 s)		Measure power (W)	Track time (s)	Efficiency (%)
	PS1 (W/m^2)	P_{th} (W)				PS2 (W/m^2)	P_{th} (W)			
DOA	(1000,1000,1000)	747	747	0.1	100.00	(850,850,850)	637	637	1.0	100.00
HGWOSCO			746.2	0.22	99.89			596.1	1.08	93.57
GOA			743.9	0.39	99.58			612.76	1.03	96.19
DFO			746.7	0.25	99.95			598.2	1.05	93.90
PSOGS			724.2	0.6	96.94			632.57	1.06	99.30
PSO			745	0.9	99.73			596.3	1.3	93.61
CSA			746.3	0.6	99.90			597	1.07	93.72
P&O			715	0.2	95.71			637	1.0	100.00
INC			584.1	0.15	78.19			417.3	1.1	65.51

Case 4. Dynamic PSCs

Fig. 12a, b shows the PV output actual power under dynamic PSCs. This condition means the solar PV modules receive time variant irradiances where the irradiances was [1000,900,800] for certain periodic time [0–1 s] as depicted in Fig. 12a, resulting in multiple local peaks and one global peak with power and voltage values of 637 W and 93.4 V as depicted in Fig. 12b. After that the irradiances changed to [900,400,1000] for another periodic time [1–2 s]. This means that the PSC changed to another PSC and the change in irradiances versus time will lead to a new global peak with power and voltage values of 460 W and 60 V as depicted in Fig. 10a,b.

In the third experiment, this is a strong PS condition where the solar radiation varies between the panels with the following values: [1000,900,800], and [900,400,1000] W/m^2. In this configuration (Fig. 13a), the DOA technique works very well, tracking the MPP in less than 0.40 s, with an efficiency of almost 99.98 %. It also reaches an MPP of 636.9 W at the first PS [1000,900,800], with a voltage of 145.3 V at MPP and a current of 4.98 A at MPP. By adjusting the irradiances to PS2: [900,400,1000], the DOA can also follow the global maximum power with reduced oscillations and in less time—just 1.30 s—to identify the peak power of 460 W achieving an astounding efficiency of over 99.65 %. With a voltage of 101 V and a current of 5.6 A at MPP, the DOA technique additionally accomplishes an MPP of 459 W. In contrast, the GOA algorithm (Fig. 13b) shows a much slower convergence time of 0.248 s and obtained at a lower value of 634.9 W at MPP, with a voltage of 138.25 V and a current of 4.6 A. This results in an efficiency of 99.67 % at the PS1 [1000,900,800]. Once the irradiances are changed to PS2: [900,400,1000], the GOA method remains at the same location as PS1 and is unable to detect the new GMPP of PS2. Comparably, the MPP is tracked by the HGWOSCO, DFO, PSOGS, PSO, CSA P&O, and INC (Fig. 13c–i) algorithms; however, their settling times are marginally longer than those of DOA. Moreover, the algorithms HGWOSCO, DFO, PSOGS, PSO, CSA P&O, and INC (Fig. 13c–i) perform poorly because they converge to the MPP much more slowly, leading to greater total power losses. In summary, the DOA method performs better in a strong PS scenario in terms of settling time and efficiency than the HGWOSCO, DFO, PSOGS, PSO, CSA P&O, and INC (Fig. 13c–i) algorithms. Table 7 shows the comparison between the obtained results during case four.

6. Experimental results and discussion section

To validate the simulation outcomes, hardware-in-loop (HIL) testing platforms were employed, as depicted in Fig. 14. The experimental setup is configured to evaluate the performance of the proposed DOA strategy under diverse dynamic and static environmental conditions, encompassing uniform and nonuniform irradiance, as well as partial shading scenarios. The control methodology is executed using NI PXIE-1071, with the hardware-in-loop simulation conducted through NI PXIE-1071 employing HIL software. The power circuit, comprising the PV array, boost converter, and load, is implemented using the FPGA board of NI PXIE-1071. The results are displayed on the power analyzer by connecting an external port board to specific ports defined in NI PXIE-1071, with a sampling frequency of 10 kHz.

In the primary scenario, the simulation model of PV modules depicts a condition without any shading. In this setup, each PV panel (G1, G2, G3) is exposed to an identical irradiation level of 1000 W/m^2, leading to the production of uniform currents. Consequently, the P-V curve exhibits a singular peak representing the global peak, commonly known as GMPP.

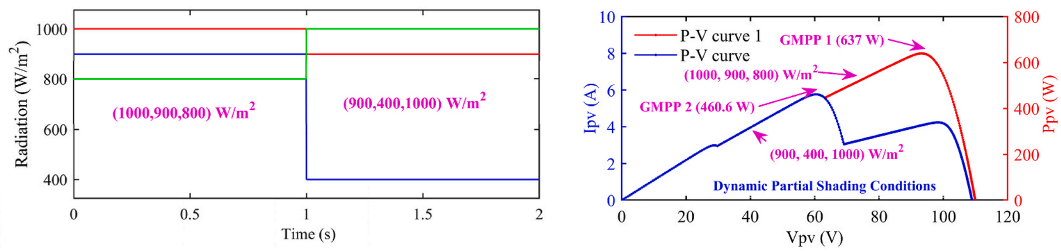

Fig. 12. P-V plots were obtained under Dynamic PSC: (a) Dynamic PSC profile, (b) P-V power curves.

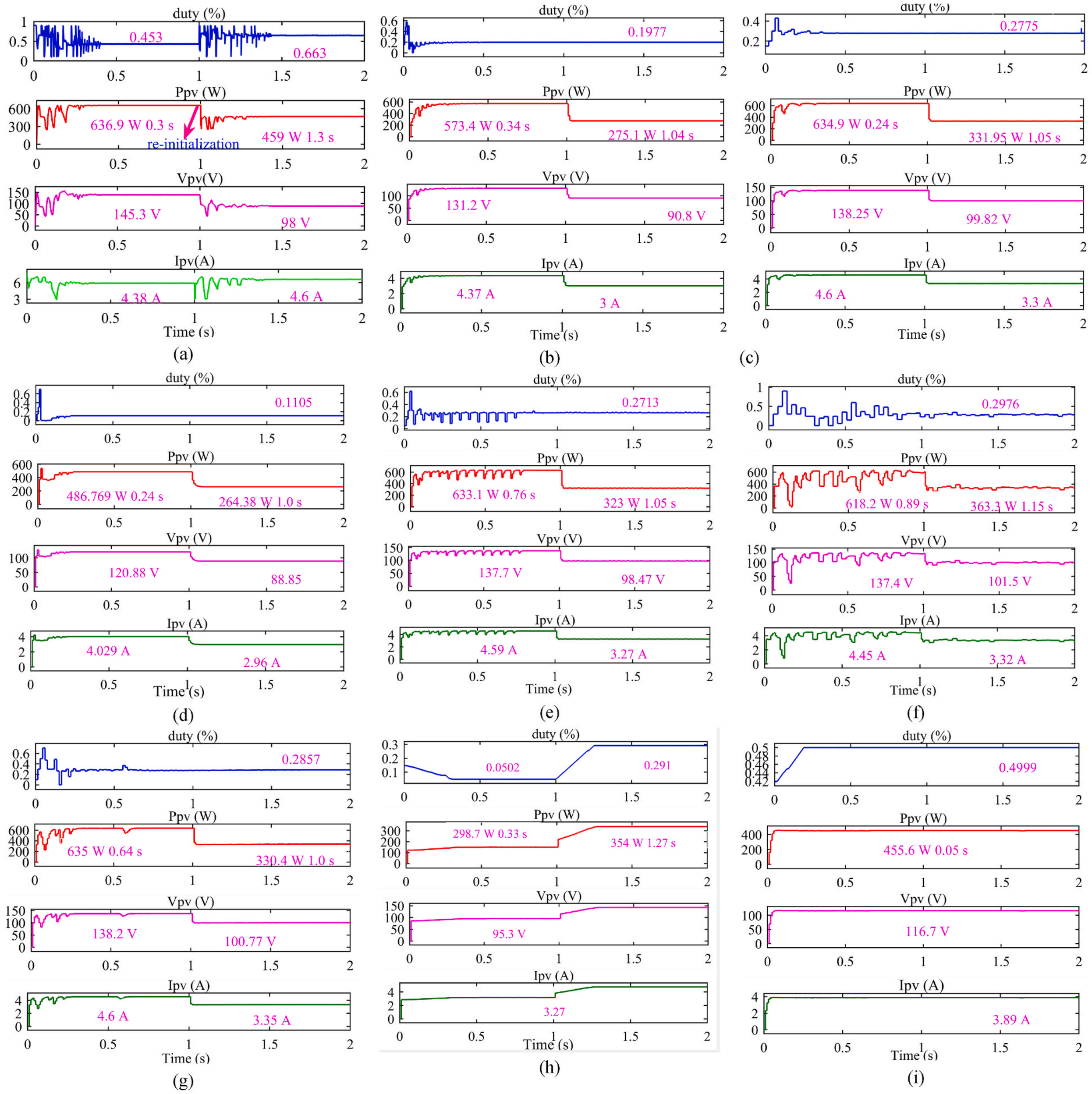

Fig. 13. The PV modules output characteristics during dynamic PSCs [1000,900,800] and [900,400,1000]: a) DOA, and b) HGWOSCO, c) GOA, d) DFO, e) PSOGS, f) PSO, g) CSA, h) P&O and i) INC.

In this experiment, the PV panels receive a consistent radiation of 1000 W/m^2. The findings indicate that DOA demonstrates a notably shorter convergence time and minimal size fluctuations (Fig. 15a) in comparison to HGWOSCO, GOA, DFO, PSOGS, PSO, CSA P&O, and INC (Fig. 15b–i) algorithms. As shown in Fig. 15a, DOA successfully detects the 745.82 W MPP at a voltage of 145.5 V and a current of 5.1 A at MPP. This results in a monitoring efficiency of 99.84 % and an estimated converging time of 0.15 s. HGWOSCO exhibits competence in exploring and exploiting new areas, managing to track the MPP at 743.62 W with a voltage of 147.70 V and a current of 5.0 A at MPP, achieving a tracking efficiency of 99.54 %. However, it takes longer to settle compared to DOA, with a settling time of 0.25 s (Fig. 15b). The comparison between GOA and DOA highlights the latter's superior performance in terms of tracking time, achieving a significantly quicker settling time. DOA attains a lower MPP value of 743.82 W with a current of 5.33 A at MPP and a voltage of 139.5 V, resulting in an efficiency of 99.58 % (Fig. 15c). Unlike HGWOSCO, GOA, DFO, PSOGS, PSO, CSA P&O, and INC (Fig. 15b–i), DOA demonstrates an improvement in settling time. While DOA excels in fully insolated environments, metaheuristic algorithms are expected to perform well even in scenarios with partial shading.

In this partial shading scenario, the simulation depicts varying irradiance levels experienced by modules G1, G2, and G3, at [1000,

Table 7
Comparisons between the obtained results under dynamic partial shading conditions (Case four).

Algorithm	First Interval (0–1 s)		Measure power (W)	Track time (s)	Efficiency (%)	Second Interval (1–2 s)		Measure power (W)	Track time (s)	Efficiency (%)
	PS1 (W/m^2)	P_{th} (W)				PS2 (W/m^2)	P_{th} (W)			
DOA	(1000,900,800)	637	636.9	0.3	99.98	(900,400,1000)	460.6	459	1.3	99.65
HGWOSCO			573.4	0.34	90.01			275.1	1.04	59.72
GOA			634.9	0.24	99.58			331.95	1.05	72.06
DFO			486.8	0.24	99.67			264.38	1.0	57.34
PSOGS			633.1	0.76	96.38			323	1.05	70.12
PSO			618.2	0.89	97.04			363.3	1.15	78.87
CSA			635	0.64	99.68			330.4	1.0	71.73
P&O			298.7	0.33	46.89			354	1.27	76.85
INC			455.6	0.05	71.52			455.6	0.05	98.91

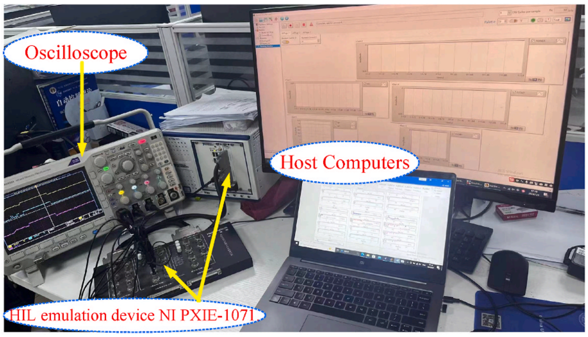

Fig. 14. HIL experimental setup.

900, 800] W/m^2, respectively. Consequently, both the shaded module and the PV string generate similar currents, although bypass diodes across each panel redirect the maximum current from the unshaded PV panels. This discrepancy in currents results in multiple peaks in the P-V curves.

In the second scenario, the three PV modules are subjected to varying radiation levels, with values of 1000, 900, and 800 W/m2, respectively. As shown in Fig. 16a, DOA adeptly tracks the MPP of 637.0 W at 138.22 V, with a current of 4.6 A at MPP, achieving a remarkable efficiency of nearly 99.85 % under partial shading conditions. Conversely, as depicted in Fig. 16c, GOA captures the MPP of 637.0 W with a current of 4.6 A at MPP and a voltage of 137.5 V at MPP, yielding an efficiency of 99.85 %, like that achieved by DOA. However, the tracking time of GOA is longer at 0.25 s. When compared to HGWOSCO, GOA, DFO, PSOGS, PSO, CSA P&O, and INC (Fig. 16b–i), DOA displays a significant improvement in settling time. These findings suggest that DOA holds several advantages over competing algorithms, particularly in terms of greater efficiency and a notable enhancement in convergence rate.

Fig. 17-a-i depicts the performance curves of the DOA, HGWOSCO, GOA, DFO, PSOGS, PSO, CSA P&O, and INC algorithms under different shading scenarios, illustrating the impact of dynamic variations in radiation on the PV modules. This simulation mirrors situations where partial shading, caused by factors such as passing clouds, intermittently affects the PV array's surface.

Under condition 1 [1000, 1000, 1000] W/m^2, with a theoretical power of 747 W, the DOA achieves an I_{mpp} of 5.1 A and V_{mpp} of 145.22 V. It obtains a P_{mpp} of 747.0 W and an efficiency of 100.00 %, with a converging time of 0.1 s as shown in Fig. 17a. Meanwhile, under the same condition (Fig. 17b), the HGWOSCO algorithm attains an I_{mpp} of 5.0 A and V_{mpp} of 146.5 V, with a P_{mpp} of 746.8 W and an efficiency of 99.97 %, requiring a tracking time of 0.35 s as shown Fig. 17b. Fig. 17a illustrates that DOA successfully tracks the first global maximum power with fewer oscillations and in less tracking time, reaching the global peak power of 747 W comparing to HGWOSCO, GOA, DFO, PSOGS, PSO, CSA P&O, and INC algorithms during dynamic uniform conditions.

In condition 2, with changed irradiances to [850, 850, 850] W/m^2, and a theoretical power of 637.0 W, the DOA achieves an efficiency of 100.00 %, tracking the P_{mpp} with a tracking time of 1.25 s at 645.0 W, and an I_{mpp} value of 4.66 A and V_{mpp} of 136.6 V. In comparison, the HGWOSCO algorithm achieves an I_{mpp} of 4.4 A and V_{mpp} of 132.5 V, with a P_{mpp} of 595.8 W and an efficiency of 93.53 %, requiring a tracking time of 1.55 s. Fig. 17c–i illustrates the performance characteristics (power, voltage and current) curves of the GOA, DFO, PSOGS, PSO, CSA P&O, and INC algorithms respectively. Additionally, the DOA exhibits consistent output power, voltage, and current even in the face of abrupt variations in solar irradiation. This discovery implies that the dynamic uniform circumstances are skillfully adapted to by the DOA-based MPPT controller, increasing the probability of achieving the optimum power point via both local and global exploration.

Fig. 18a–i depicts the performance curves of the HGWOSCO, GOA, DFO, PSOGS, PSO, CSA P&O, and INC algorithms under dynamic partial shading (DPS), illustrating the impact of dynamic of PSC on the PV array. DPS conditions refer to situations in which solar photovoltaic (PV) panels experience varying levels of shading over time. Shading occurs when some parts of the PV array are

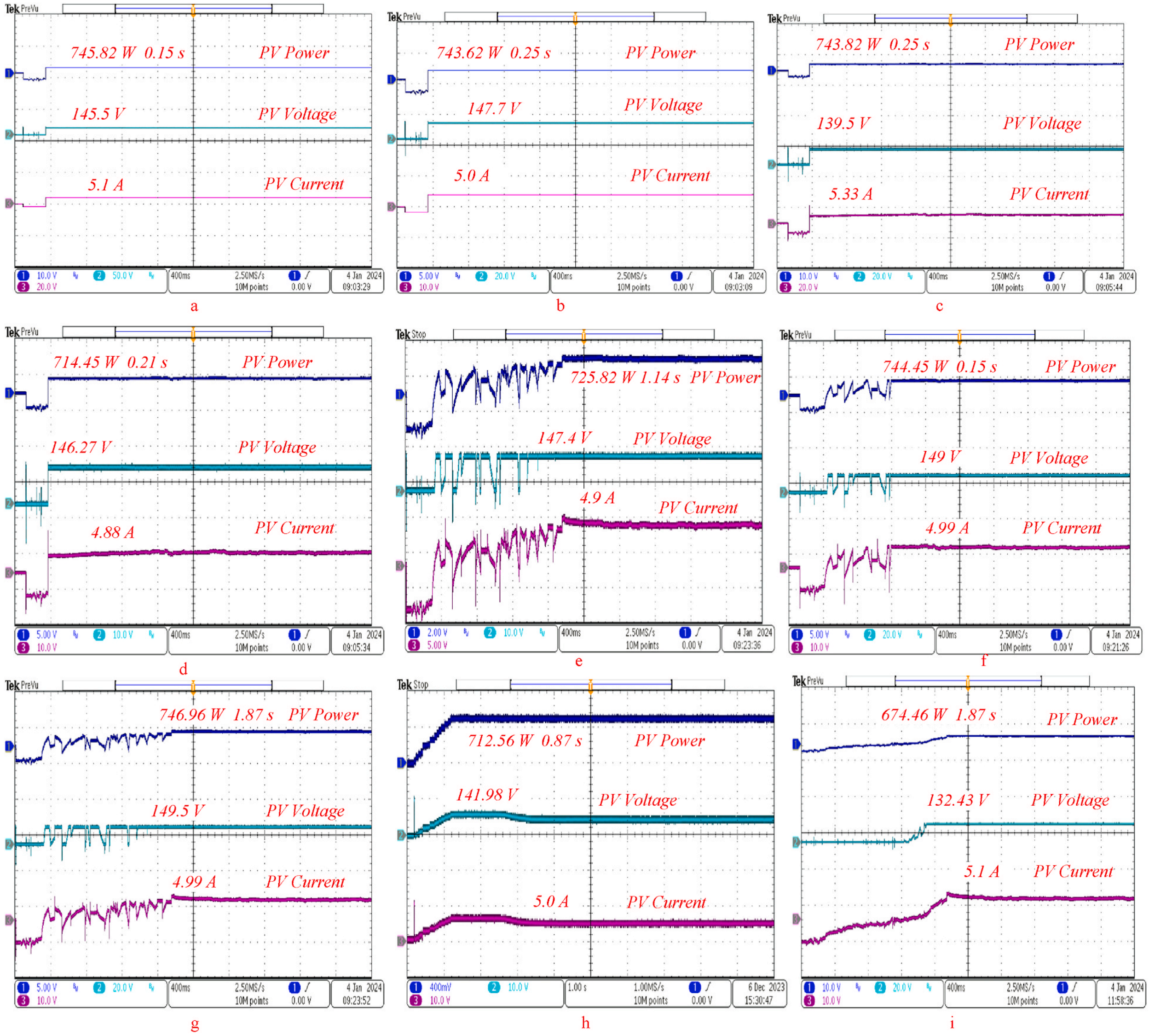

Fig. 15. The PV modules output characteristics during static uniform weather conditions [1000, 1000, 1000]: a) DOA, and b) HGWOSCO, c) GOA, d) DFO, e) PSOGS, f) PSO, g) CSA, h) P&O and i) INC.

exposed to sunlight, while others are shaded due to objects such as buildings, trees, or other obstructions. This dynamic shading can occur throughout the day as the sun's position changes, or due to moving objects like clouds.

Under DPS1 [1000, 900, 800] W/m^2, with a theoretical power and voltage of 637 W and 93.4 V, the DOA achieves an I_{mpp} of 5.4 A and V_{mpp} of 135.22 V as well as it obtains a P_{mpp} of 630.188 W and an efficiency of 98.93 %, with a converging time of 0.3 s as shown Fig. 18a. Meanwhile, under the same condition, the GOA algorithm accomplishes an I_{mpp} of 4.6 A and V_{mpp} of 137.5 V, with a P_{mpp} of 632.5 W and an efficiency of 99.29 %, requiring a tracking time of 0.65 s as shown Fig. 18c. Fig. 18a illustrates that DOA successfully tracks the first global maximum power with fewer oscillations and in less tracking time, reaching the global peak power of 637 W comparing to the HGWOSCO, GOA, DFO, PSOGS, PSO, CSA P&O, and INC algorithms under dynamic partial shading (DPS),

In DPS 2, [900, 400, 1000] W/m^2, and a theoretical power and voltage of 460.6W and 60 V, the DOA achieves a efficiency of 94.49 %, tracking the P_{mpp} with a time of 1.25 s at 435.24 W, and an I_{mpp} value of 3.9 A and V_{mpp} of 111.6 V. In comparison, the GOA algorithm accomplishes an I_{mpp} of 3.4 A and V_{mpp} of 97.5 V, with a P_{mpp} of 331.5 W and an efficiency of 71.97 %, requiring a tracking time of 1.33 s. Notably, the obtained results in terms of the efficiency and tracking time of each techniques and the ability of each technique to extract the highest power in the shortest possible time, DOA successfully tracks the first global maximum power with fewer oscillations and in less tracking time, reaching the global peak power of 637 W comparing to the HGWOSCO, GOA, DFO, PSOGS, PSO, CSA P&O, and INC algorithms under dynamic partial shading (DPS).

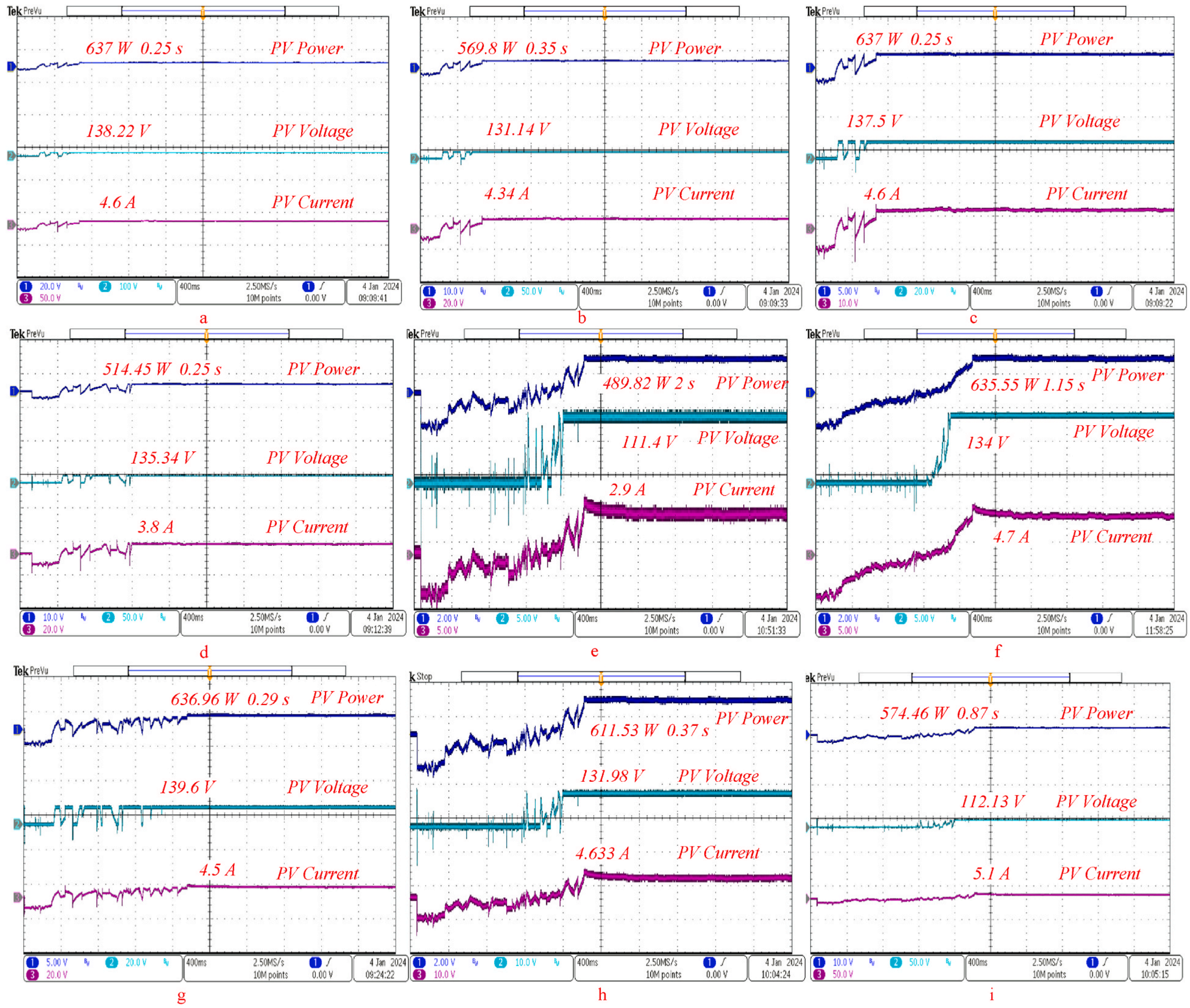

Fig. 16. The PV modules output characteristics during static PSCs [1000, 900, 800]: a) DOA, and b) HGWOSCO, c) GOA, d) DFO, e) PSOGS, f) PSO, g) CSA, h) P&O and i) INC.

7. The MPPT algorithms' performance discussion

The potential of an MPPT approach to precisely trace the Maximum Power Point (MPP) of a photovoltaic (PV) system is crucial for assessing its performance under both static and dynamic conditions, including uniform and partially shaded scenarios. Accurate MPP tracking ensures that the PV system operates at its highest possible efficiency, even when subjected to challenging conditions such as partial shading, which can significantly reduce overall system efficiency.

7.1. Key variables for assessing MPPT effectiveness

Accuracy of Tracking: This variable measures the effectiveness of the MPPT approach in tracking the PV system's MPP during partial shading conditions (PSC). It is typically expressed as a percentage of the PV system's total power output that the MPPT approach successfully tracks. High accuracy indicates that the algorithm can closely follow the true MPP, minimizing power losses due to shading.

MPPT Speed: The speed of the MPPT mechanism is critical, especially under dynamic PSC, where irradiance levels can change rapidly. MPPT speed is defined as the time required for the MPPT method to adjust its tracking parameters to align with the new MPP. A faster response time ensures that the PV system quickly adapts to changing conditions, maintaining optimal power output.

Stability: Stability refers to the MPPT technique's ability to consistently follow the PV system's MPP without oscillations or deviations, even during dynamic PSC. A stable MPPT method ensures reliable performance and avoids fluctuations that can cause inefficiencies or damage to the system.

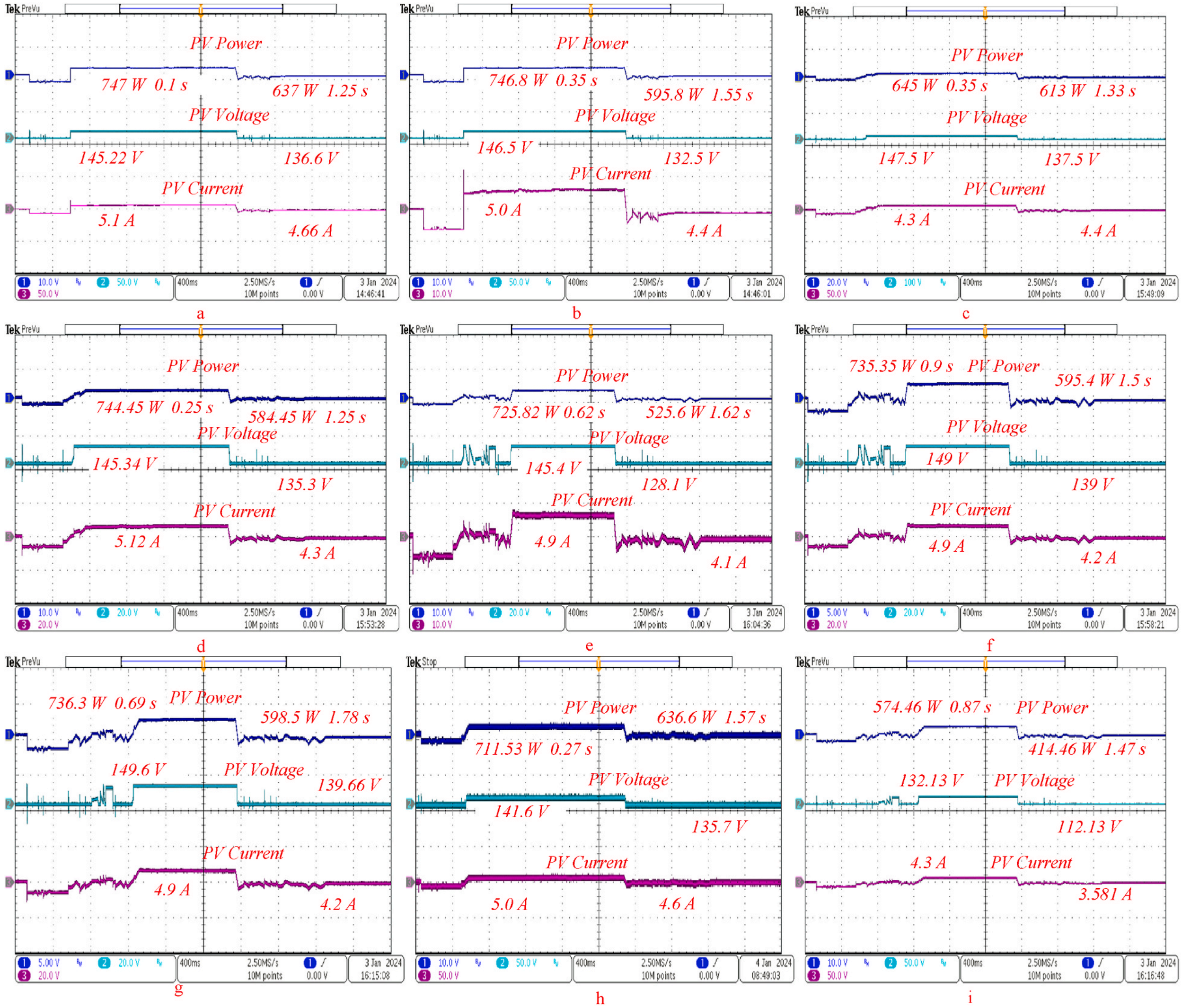

Fig. 17. The PV modules output characteristics during dynamic uniform conditions [1000,1000,1000] and [850,850,850]: a) DOA, and b) HGWOSCO, c) GOA, d) DFO, e) PSOGS, f) PSO, g) CSA, h) P&O and i) INC.

7.2. Evaluation of the DOA-based MPPT approach

In this study, we evaluated the effectiveness of the proposed Dandelion Optimizer Algorithm (DOA)-based MPPT approach by summarizing the average efficiency and tracking time for various algorithms. The results, depicted in Fig. 19, demonstrate that the DOA-based method provides a robust solution for MPP tracking, outperforming traditional algorithms in both static and dynamic scenarios.

The comprehensive evaluation included comparisons with other state-of-the-art algorithms, highlighting the DOA's superior performance in terms of accuracy, speed, and stability. These findings underscore the DOA's potential as a reliable and efficient method for optimizing PV system performance under varying environmental conditions.

In addition to statistical validation, future research will explore the integration of the DOA-based MPPT method with other advanced techniques and real-world PV systems. This will include field testing under diverse environmental conditions to assess the practical feasibility and robustness of the approach.

8. Conclusions

The implementation of the Dandelion Optimizer Algorithm (DOA) method in Maximum Power Point Tracking (MPPT) controllers offers a promising strategy to enhance the effectiveness and reliability of solar photovoltaic (PV) systems under both static and dynamic conditions, including uniform and non-uniform (partial shading) scenarios. The DOA approach effectively balances the trade-offs between tracking speed, precision, and convergence, making it a robust solution for optimizing power output. By dynamically

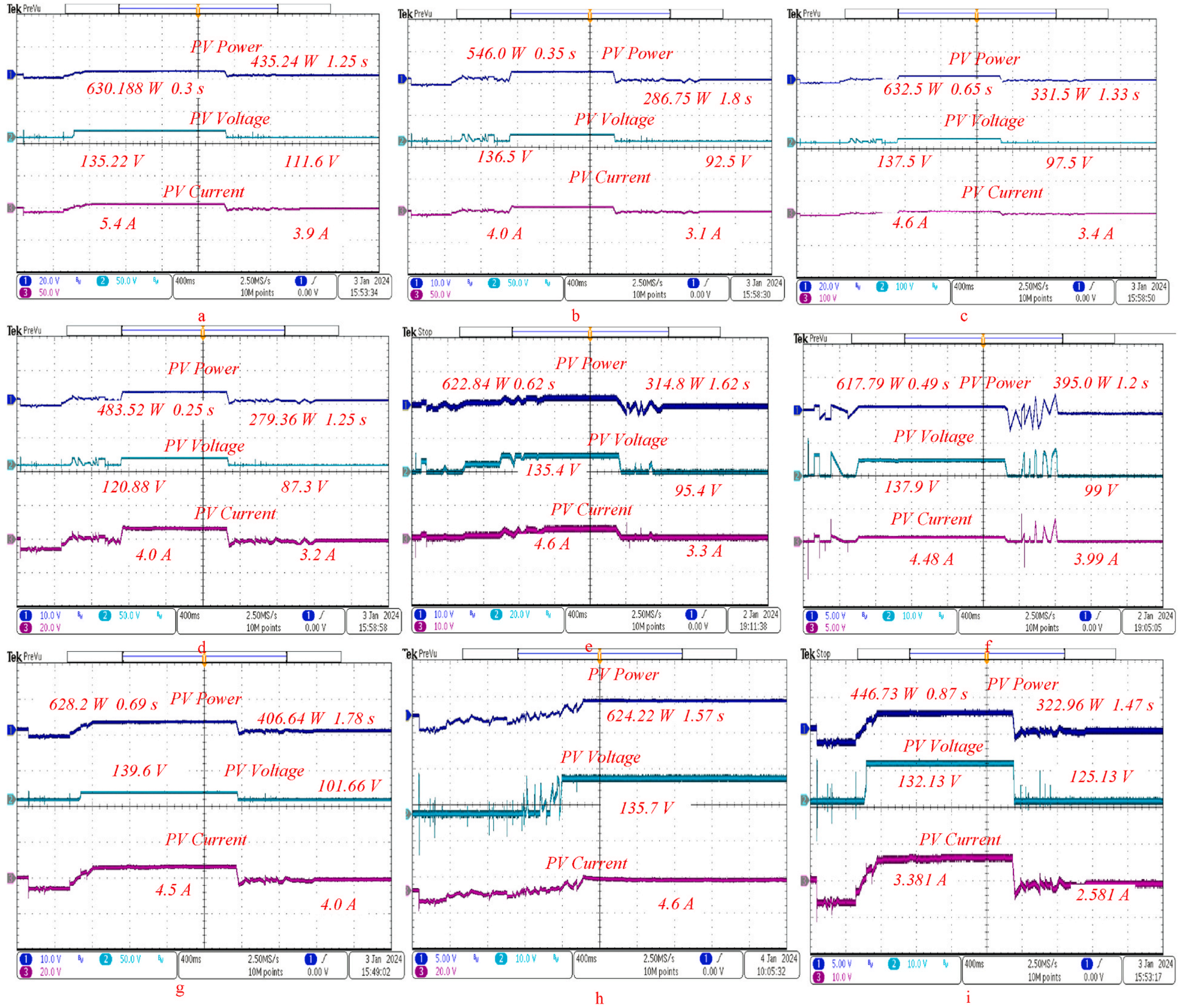

Fig. 18. Obtained results for CSO and PSO under dynamic PSCs: [1000, 900, 800] to [1000, 400, 900]: a) DOA, and b) HGWOSCO, c) GOA, d) DFO, e) PSOGS, f) PSO, g) CSA, h) P&O and i) INC.

adjusting to varying irradiance levels and shading patterns, the DOA method ensures that the PV system operates at its optimal performance, thereby maximizing energy harvest and improving overall system efficiency. This makes the DOA an advantageous choice for addressing the challenges posed by partial shading and other dynamic environmental factors in solar PV applications. The MPPT-based DOA approach beats other commonly employed MPPT-based metaheuristic techniques, including HGWOSCO, GOA, DFO, PSOGS, PSO, CSA P&O, and INC, as proved by the trials presented in this scientific publication, confirming its supremacy. The obtained results show that the DOA approach works better than HGWOSCO, GOA, DFO, PSOGS, PSO, CSA P&O, and INC algorithms. On average, the DOA approach accomplishes a tracking time of 0.5 s and an efficiency of 99.93 %. In evaluation, the HGWOSCO, GOA, DFO, PSOGS, PSO, CSA P&O, and INC algorithms take tracking time of 0.535 s, 0.525 s, 0.48 s, 1.01 s, 1.14 s, 0.704 s, 0.56 s and 0.251 s respectively, with an efficiency of 88.84 %, 94.48 %, 87.12 %, 88.05 %, 94.79 %, 93.82 %, 85.25 % and 77.93 % respectively. Furthermore, the benefits of the DOA method are confirmed by simulation study performed using a hardware-in-the-loop (HIL) NI PXIE-1071 simulator. The acquired results show that, even in difficult situations involving static and dynamic uniform irradiance and PSCs, the proposed DOA-based MPPT technique is dependable, well-organized, precise, and quick. This study demonstrates the DOA technique's capacity to successfully accomplish its goals.

The performance of the DOA methodology in grid-connected PV systems and its applicability to MPPT techniques for other renewable energy sources, such wind and hydro, may be investigated in more detail. These studies would advance our knowledge of and ability to use DOA in a variety of renewable energy applications.

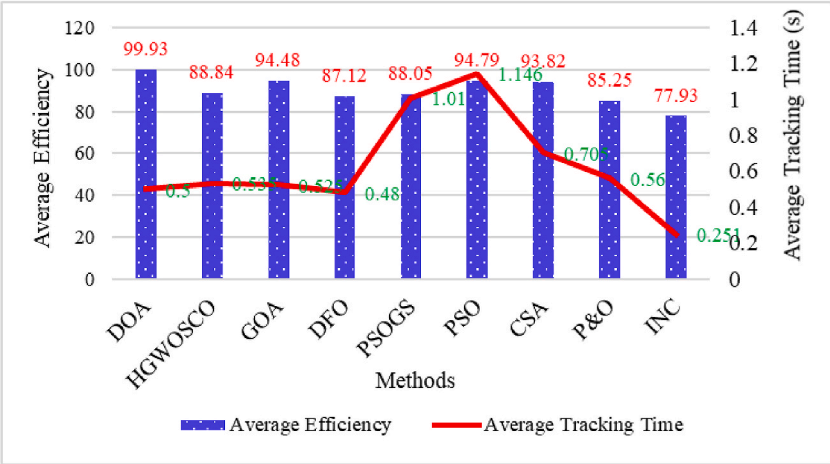

Fig. 19. Comparative analysis of evaluation parameters for all simulation cases.

Data availability

The data is not shared but the data will be available if requested by the journal.

Ethics approval

Not applicable, because this article does not contain any studies of human or animal subjects.

Consent to participate

Not applicable.

Consent for publication

Not applicable.

CRediT authorship contribution statement

Hassan M. Hussein Farh: Writing – review & editing, Visualization, Validation, Supervision, Software, Ibrahim AL-Wesabi, Writing – review & editing, Writing – original draft, Visualization, Validation, Supervision, Software, Resources. **Zhijian Fang:** Writing – review & editing, Validation, Supervision, Software. **Fahad Alaql:** Writing – review & editing, Writing – original draft, Visualization, Investigation, Xu Jiazhu, Writing – review & editing, Writing – original draft, Software, Methodology, Investigation, Abdullrahman A. A. Al-Shamma'a, Writing – review & editing, Writing – original draft, Visualization, Validation, Supervision, Resources, Methodology, Investigation. **Walied Alfraidi:** Writing – original draft, Visualization, Validation. **Muhammad Hamza Zafar:** Writing – review & editing, Writing – original draft, Validation, Supervision, Software.

Declaration of competing interest

The authors declare that they have no known competing financial interests or personal relationships that could have appeared to influence the work reported in this paper.

Acknowledgements

The authors extend their appreciation to the Deputyship for Research & Innovation, Ministry of Education in Saudi Arabia for funding this research through the project number IFP-IMSIU-2023074. The authors also appreciate the Deanship of Scientific Research at Imam Mohammad Ibn Saud Islamic University (IMSIU) for supporting and supervising this project.

References

[1] I. Al-wesabi, F. Zhijian, C. Jiuqing, H.M. Hussein, I. Aboudrar, I. Dagal, T. Kandil, A.A. Al-shamma, F. Saeed, International Journal of Hydrogen Energy Fast DC-link voltage control based on power flow management using linear ADRC combined with hybrid salp particle swarm algorithm for PV/wind energy conversion system, Int. J. Hydrogen Energy 61 (2024) 688–709, https://doi.org/10.1016/j.ijhydene.2024.02.325.

[2] I. Al-Wesabi, F. Zhijian, H.M.H. Farh, I. Dagal, A.A. Al-Shamma'a, A.M. Al-Shaalan, Y. kai, Hybrid SSA-PSO based intelligent direct sliding-mode control for extracting maximum photovoltaic output power and regulating the DC-bus voltage, Int, J. Hydrogen Energy (2023), https://doi.org/10.1016/j.ijhydene.2023.10.034.

[3] H. Özbay, S. Öncü, M. Kesler, SMC-DPC based active and reactive power control of grid-tied three phase inverter for PV systems, Int. J. Hydrogen Energy 42 (2017) 17713–17722, https://doi.org/10.1016/j.ijhydene.2017.04.020.

[4] W.-J. Chen, S.-A. Farooqui, H.-D. Liu, S.-X. Lai, P.-J. Lin, Novel MPPT algorithm based on honey bees foraging characteristics for solar power generation systems, Heliyon 10 (2024) e27491.

[5] A. Beşkirli, İ. Dağ, Parameter extraction for photovoltaic models with tree seed algorithm, Energy Rep. 9 (2023) 174–185.

[6] A. Beşkirli, İ. Dağ, I-CPA: an improved carnivorous plant algorithm for solar photovoltaic parameter identification problem, Biomimetics 8 (2023) 569.

[7] S. Dadfar, K. Wakil, M. Khaksar, A. Rezvani, M.R. Miveh, M. Gandomkar, Enhanced control strategies for a hybrid battery/photovoltaic system using FGS-PID in grid-connected mode, Int. J. Hydrogen Energy 44 (2019) 14642–14660, https://doi.org/10.1016/j.ijhydene.2019.04.174.

[8] B. Dandil, H. Acikgoz, R. Coteli, An effective MPPT control based on machine learning method for proton exchange membrane fuel cell systems, Int, J. Hydrogen Energy (2024), https://doi.org/10.1016/j.ijhydene.2024.02.076.

[9] A.O. Salau, G.K. Alitasb, MPPT efficiency enhancement of a grid connected solar PV system using Finite Control set model predictive controller, Heliyon 10 (2024) e27663.

[10] I. Al-Wesabi, F. Zhijian, H.M.H. Farh, W. Zhiguo, K. Ameur, A.A. Al-Shamma'a, A.M. Al-Shaalan, Dynamic global power extraction of partially shaded PV system using a hybrid MPSO-PID with anti-windup strategy, Eng. Appl. Artif. Intell. 126 (2023) 106965, https://doi.org/10.1016/J.ENGAPPAI.2023.106965.

[11] S.A. Hamad, M.A. Ghalib, Fuzzy MPPT operation-based model predictive flux control for linear induction motors, Int. J. Hydrogen Energy 50 (2024) 1035–1044, https://doi.org/10.1016/j.ijhydene.2023.10.051.

[12] H.B. Percin, A. Caliskan, Whale optimization algorithm based MPPT control of a fuel cell system, Int. J. Hydrogen Energy 48 (2023) 23230–23241, https://doi.org/10.1016/j.ijhydene.2023.03.180.

[13] A. Saxena, R. Kumar, M. Amir, S.M. Muyeen, Maximum power extraction from solar PV systems using intelligent based soft computing strategies: a critical review and comprehensive performance analysis, Heliyon 10 (2023) e22417.

[14] I. Al-Wesabi, Z. Fang, Z. Wei, H. Dong, Direct sliding mode control for dynamic instabilities in dc-link voltage of standalone photovoltaic systems with a small capacitor, Electron 11 (2022), https://doi.org/10.3390/electronics11010133.

[15] A. Laib, F. Krim, B. Talbi, H. Feroura, A. Belaout, Hardware implementation of fuzzy maximum power point tracking through sliding mode current control for photovoltaic systems, Rev. Roum. Des Sci. Tech. Ser. Electrotech. Energ 66 (2021) 91–96.

[16] B. Talbi, F. Krim, T. Rekioua, A. Laib, H. Feroura, Design and hardware validation of modified P&O algorithm by fuzzy logic approach based on model predictive control for MPPT of PV systems, J. Renew. Sustain. Energy 9 (2017), https://doi.org/10.1063/1.4999961.

[17] D.J.K. Kishore, M.R. Mohamed, K. Sudhakar, K. Peddakapu, A new meta-heuristic optimization-based MPPT control technique for green energy harvesting from photovoltaic systems under different atmospheric conditions,, Environ. Sci. Pollut. Res. 30 (2023) 84167–84182, https://doi.org/10.1007/s11356-023-28248-8.

[18] I. Al-Wesabi, Z. Fang, H.M. Hussein Farh, A.A. Al-Shamma'a, A.M. Al-Shaalan, Comprehensive comparisons of improved incremental conductance with the state-of-the-art MPPT Techniques for extracting global peak and regulating dc-link voltage, Energy Rep. 11 (2024) 1590–1610, https://doi.org/10.1016/j.egyr.2024.01.020.

[19] H.M.H. Farh, A.A. Al-Shamma'a, Maximum Power Extraction from Partially Shaded Photovoltaic Power Conversion Systems, (n.d.).

[20] H.M.H. Farh, A. Fathy, A.A. Al-Shamma'a, S. Mekhilef, A.M. Al-Shaalan, Global research trends on photovoltaic maximum power extraction: systematic and scientometric analysis, Sustain. Energy Technol, Assessment 61 (2024) 103585.

[21] R. Kahani, M. Jamil, M.T. Iqbal, An improved perturb and observed maximum power point tracking algorithm for photovoltaic power systems, J. Mod. Power Syst. Clean Energy 11 (2023) 1165–1175, https://doi.org/10.35833/MPCE.2022.000245.

[22] S. Ahmed, S. Mekhilef, M. Mubin, K.S. Tey, M. Kermadi, An adaptive perturb and observe algorithm with enhanced skipping feature for fast global maximum power point tracking under partial shading conditions, IEEE Trans. Power Electron. 38 (2023) 11601–11613.

[23] I. Al-Wesabi, F. Zhijian, H.M. Hussein Farh, A.A. Al-Shamma'a, H. Dong, A.M. Al-Shaalan, T. Kandil, Maximum power extraction and DC-Bus voltage regulation in grid-connected PV/BES system using modified incremental inductance with a novel inverter control, Sci. Rep. 12 (2022) 1–21, https://doi.org/10.1038/s41598-022-22952-0.

[24] H. Bakır, A novel artificial hummingbird algorithm improved by natural survivor method, Neural Comput. Appl. (2024) 1–25.

[25] H. Bakır, Enhanced artificial hummingbird algorithm for global optimization and engineering design problems, Adv. Eng. Software 194 (2024) 103671.

[26] A.M. Eltamaly, H.M.H. Farh, Dynamic global maximum power point tracking of the PV systems under variant partial shading using hybrid GWO-FLC, Sol. Energy 177 (2019) 306–316, https://doi.org/10.1016/j.solener.2018.11.028.

[27] H. Bakır, Comparative performance analysis of metaheuristic search algorithms in parameter extraction for various solar cell models, Environ. Challenges 11 (2023) 100720.

[28] K. Khan, S. Rashid, M. Mansoor, A. Khan, H. Raza, M.H. Zafar, N. Akhtar, Data-driven green energy extraction: machine learning-based MPPT control with efficient fault detection method for the hybrid PV-TEG system, Energy Rep. 9 (2023) 3604–3623, https://doi.org/10.1016/J.EGYR.2023.02.047.

[29] E. Halassa, L. Mazouz, A. Seghiour, A. Chouder, S. Silvestre, Revolutionizing photovoltaic systems: an innovative approach to maximum power point tracking using enhanced dandelion optimizer in partial shading conditions, Energies 16 (2023), https://doi.org/10.3390/en16093617.

[30] N. Kacimi, A. Idir, S. Grouni, M.S. Boucherit, Improved MPPT control strategy for PV connected to grid using IncCond-PSO-MPC approach, CSEE J, Power Energy Syst 9 (2023) 1008–1020, https://doi.org/10.17775/CSEEJPES.2021.08810.

[31] I. Al-Wesabi, Z. Fang, H.M.H. Farh, A.A. Al-Shamma'a, A.M. Al-Shaalan, T. Kandil, M. Ding, Cuckoo search combined with PID controller for maximum power extraction of partially shaded photovoltaic system, Energies 15 (2022) 2513.

[32] A.M. Eltamaly, A novel musical chairs algorithm applied for MPPT of PV systems, Renew, Sustain. Energy Rev 146 (2021) 111135, https://doi.org/10.1016/j.rser.2021.111135.

[33] M.H. Zafar, N.M. Khan, A.F. Mirza, M. Mansoor, Bio-inspired optimization algorithms based maximum power point tracking technique for photovoltaic systems under partial shading and complex partial shading conditions, J. Clean. Prod. 309 (2021) 127279, https://doi.org/10.1016/j.jclepro.2021.127279.

[34] I. Sajid, A. Gautam, A. Sarwar, M. Tariq, H.D. Liu, S. Ahmad, C.H. Lin, A.E. Sayed, Optimizing photovoltaic power production in partial shading conditions using dandelion optimizer (DO)-Based MPPT method, Processes 11 (2023), https://doi.org/10.3390/pr11082493.

[35] S. Mohanty, B. Subudhi, P.K. Ray, A new MPPT design using grey wolf optimization technique for photovoltaic system under partial shading conditions,, IEEE Trans. Sustain. Energy 7 (2015) 181–188.

[36] S. Titri, C. Larbes, K.Y. Toumi, K. Benatchba, A new MPPT controller based on the Ant colony optimization algorithm for Photovoltaic systems under partial shading conditions,, Appl. Soft Comput. 58 (2017) 465–479.

[37] H. Li, D. Yang, W. Su, J. Lü, X. Yu, An overall distribution particle swarm optimization MPPT algorithm for photovoltaic system under partial shading, IEEE Trans. Ind. Electron. 66 (2018) 265–275.

[38] A. Ibrahim, M.B. Shafik, M. Ding, M.A. Sarhan, Z. Fang, A.G. Alareqi, T. Almoqri, A.M. Al-Rassas, PV maximum power-point tracking using modified particle swarm optimization under partial shading conditions, Chinese J. Electr. Eng 6 (2020) 106–121.

[39] G. Al-Muthanna, S. Fang, I. Al-Wesabi, K. Ameur, H. Kotb, K.M. AboRas, H.Z.A. Garni, A.A. Mas'ud, A high speed MPPT control utilizing a hybrid PSO-pid controller under partially shaded photovoltaic battery chargers,, Sustain. Times 15 (2023), https://doi.org/10.3390/su15043578.
[40] A. Ibrahim, Fast DC-Link Voltage Regulation, Maximum Power, Extraction for standalone PV/BES system using hybrid SPSA-DSMC, 2023 IEEE Energy Convers. Congr. Expo (2023) 427–433, https://doi.org/10.1109/ECCE53617.2023.10362571.
[41] A.M. Eltamaly, M.S. Al-Saud, A.G. Abokhalil, A novel scanning bat algorithm strategy for maximum power point tracker of partially shaded photovoltaic energy systems, Ain Shams Eng. J. 11 (2020) 1093–1103.
[42] M. Mansoor, A.F. Mirza, Q. Ling, M.Y. Javed, Novel Grass Hopper optimization based MPPT of PV systems for complex partial shading conditions, Sol. Energy 198 (2020) 499–518.
[43] A.M. Eltamaly, An improved cuckoo search algorithm for maximum power point tracking of photovoltaic systems under partial shading conditions, Energies 14 (2021) 953.
[44] C. González-Castaño, C. Restrepo, S. Kouro, J. Rodriguez, MPPT algorithm based on artificial bee colony for PV system, IEEE Access 9 (2021) 43121–43133.
[45] A. Ibrahim, M. Ding, X. Jin, X. Dai, M.A. Sarhan, M.B. Shafik, H. Zhou, Artificial neural network based maximum power point tracking for PV system, in: 2019 Chinese Control Conf., IEEE, 2019, pp. 6559–6564.
[46] S. Zhao, T. Zhang, S. Ma, M. Chen, Dandelion Optimizer: a nature-inspired metaheuristic algorithm for engineering applications,, Eng. Appl. Artif. Intell. 114 (2022) 105075.